Effect of excess Sodium (Na) on Barium (Ba),Cobalt (Co) and Cadmium (Cd) emission during ICP-OES: Simulation on the basis of the simplified rate model.

A THESIS SUBMITTED IN PARTIAL FULFILMENT OF THE REQUIREMENTS OF THE MASTER OF SCIENCE IN ANALYTICAL CHEMISTRY DEGREE.

BY GLADMORE RONGAI

UNIVERSITY OF ZIMBABWE

FACULTY OF SCIENCE

CHEMISTRY DEPARTMENT

P.O BOX MP 167

MOUNT PLEASANT

HARARE

2015

Acknowledgements

I would like to thank my supervisor Professor MF Zaranyika for his guidance and motivation. I also wish to thank my family for theirsupport and continuous inspiration. My former employer SAZ deserves special mention for availing the laboratory equipment to me. Finally I would like to thank God for sailing with me.

Dedication

This work is dedicated to my late parents who have imparted an education legacy on me. My family members, Gregory, Gabriel, Georgina, Gloria, Geneniaand Biggie for encouraging me to go on and on.

ABSTRACT

The effects of excess Sodium (Na) on Cobalt (Co), Cadmium (Cd) and Barium (Ba) were studied using the inductively coupled plasma-optical emission spectrometry (ICP-OES). The emission signals of the analytes with the inteferent were evaluated as E'/E and plotted against the concentration. Readings were taken between 0-10mg/l for Cobalt and Cadmium whilst for Barium; readings were taken from 0-30mg/l. The experimental graphs revealed that there is an effect of the intereferent on the signal emission. Comparisons were made using the theoretically calculated graphs from which a derivative and applicable theory to explain the experimental graphs was simulated. The theories explained variables in which $\Delta E = 0$, $\Delta E = IP\ (int) - IP\ (anal)$ and $\Delta E = kt - IP\ (anal)$ in which ΔE is the change in energy. These were used to simulate the relationship between the experimental and the theoretical graphs. However a close relationship was realised between the graphs.

TABLE OF CONTENTS

Contents **Page**

CHAPTER 1.INTRODUCTION…………………………………………………………….…....1

1.1Background……………………………………………………………………….…….1

1.2 Statement of the problem………………………………………………….……...2

1.3 Objectives/Aims………………………………………………….………….2

CHAPTER 2.LITERATURE REVIEW…………………………………………….……....3

2.1Principles of Inductively coupled plasma ………………………..……..…...…..….3

2.1.1Advantages of using Argon……………………………………….………...…..…4

2.1.2 Disadvantages of using Argon…………………………………………...….…...5

2.2Formation of ICP…………………..……………………………………..…......6

2.2.1Zones of the plasma…………………………………………….………7

2.2.2Configuration of the ICP Torch……………………………….……...…8

2.2.2.1Radial view and Axial view………………………………..…….….…..8

2.2.2.2 Disadvantages of the axial view...….……………………...……….………9

2.2.3Dual view...……..11

2.2.4.1Temperature and electron number density..…………………………..…….12

2.2.4.2Local ThermodynamicEquilibrium……………………………….…….12

2.2.4.3Departures from Thermodynamic Equilibrium..………..…….……………13

2.2.5 Ionization interference……….…………………………………..……..…..14

2.2.5.1Simplified Rate Model……………………………………………..…….16

CHAPTER 3.EXPERIMENTAL SECTION……………………...…………..………...…….15

3.0Methodology…………………………………………………………...…....17

3.1Experimental…………………………….………………………..……….17

3.2Materials……………………………………………………….…….…18

3.3Procedure………………………..……………………………………19

3.4Average Aspiration Determination…………………………………….….19

3.5Nebulization Efficiency……………………………………….….....20

3.6 Determination of Plasma Temperature………………………………………22

CHAPTER 4.THEORETICAL AND EXPERIMENTAL CALCULATIONS ….……...…....24

4.1Experimental Results ….. …………...……………………………...…….24

4.2 Theoretical Results ………………………………………………...….….29

4.2.1Total analytes atoms reaching the torch…………………….……….31

4.2.2 Analytes number density…………………………………..……....34

4.2.3Degree of ionization using the Saha equation…………….....…….…36

4.3 Graphical Presentations……………………………………………………….41

4.3.1nμ'/nμ values when ΔE =0……………………………..………..…42

4.3.2nμ'/nμ values whenΔE =IP (int) – (IP (anal)……………..…….……47

4.3.3nμ'/nμ values whenΔE =kt –IP……………………..………..…...53

CHAPTER 5. RESULTS AND DISCUSSION…………….……………………………..….59

5.1 Cobalt

5.1.1 When ΔE =0…………………………………………………...59

5.1.2 When ΔE =IP(int) – (IP(anal…………………………………..61

5.1.3 When ΔE =kt –IP……………………………….…………..62

5.2 Barium……………………………………………..…………..63

5.2.1 When ΔE =0……………………………………….…………..63

5.2.2 When ΔE =IP(int) – (IP(anal……………………….………….64

5.2.3 When ΔE =kt –IP…………………………………..………..65

5.3 Cadmium……………………………………….…..………66

5.3.1 When ΔE =0………………………………….……...……...66

5.3.2 When ΔE =IP(int) – (IP(anal)…………………….…………....67

5.3.3 When ΔE =kt –IP…………………………….………………..68

CHAPTER 6 CONCLUSION AND RECOMMENDATIONS……………………….…….…......69

6.1 Conclusions……………………………………………………………69

6.2 Recommendations ……………………………………………….…….…70

REFERENCES………………………...…….…………………………………………71

LIST OF FIGURES

Figure **Page**

Figure 1: Typical Inductive Plasma Source…………..…………………………………………...…3

Figure 2(i): The ICP Axial View………………………………………………………..….......8

Figure 2(ii): The ICP Radial View……………..……………………………………..…......9

Figure 3: A shear gas blowing away possible salt deposits to the optical interface…….….……...….10

Figure 4: E’/E Experimental Sodium interference on Barium……………………………………...25

Figure 5: E’/E Experimental Sodium interference on Cadmium……..……………………….......….27

Figure 6:E’/E Experimental Sodium interference on Cobalt….…………. …………..……………...28

Figure 7:ηύ/ημ of Theoretical Cobalt interference with Sodium when$\Delta E = 0$…………………........44

Figure 8:ηύ/ημ of Theoretical Barium interference with Sodium when $\Delta E = 0$ ……….…………....45

Figure 9:ηύ/ημ of Theoretical Cadmium interference with Sodium when $\Delta E = 0$…….………........46

Figure 10:ηύ/ημ of Theoretical Cobalt interference with Sodiumwhen ΔE = IP (int)- IP (anal…..…..50

Figure 11:ηύ/ημ of Theoretical Barium interference with Sodium when ΔE = IP (int)- IP(anal)……….51

Figure12: ηύ/ημ of Theoretical Cadmium interference with Sodium when ΔE = IP (int)- IP (anal…...52

Figure 13: ηύ/ημ of Theoretical Cobalt interference with Sodium when ΔE = kt -IP (anal)………….....56

Figure 14:ηύ/ημ of Theoretical Barium interference with Sodium whenΔE = kt -IP (anal)……………..57

Figure 15: ηύ/ημ of Theoretical Cobalt interference with Sodium whenΔE = kt -IP (anal)……………..58

Fig 16. Comparison between the theoretical and experimental values of Cobalt when ΔE =0……….59

Fig 17.Comparison between the theoretical and experimental values of Cobaltwhen ΔE =IP (int) – (IP(anal)……………………………………………………………………………………………….61

Fig 18.Comparison between the theoretical and experimental values of Cobalt when ΔE =kt – IP………………………………………………………………………………………………….....62

Fig 19: Comparison between the theoretical and experimental values of Barium when ΔE =0………………………………………………………………………………………………..….63

Fig 20: Comparison between the theoretical and experimental values of Barium when ΔE =IP (int) – IP (anal)………………………………………………………………………………...…………...64

Fig21: Comparison between the theoretical and experimental values of Barium when ΔE =kt – IP…………………………………………………………………………………………………....65

Fig22: Comparison between the theoretical and experimental values of Cadmium when ΔE =0…………………………………………………………………………………………………...66

Fig 23: Comparison between the theoretical and experimental values of Cadmium when IP (int) – IP (anal)……………………………………………………………………………………………..67

Fig 24: Comparison between the theoretical and experimental values of Cadmium when ΔE =kt – IP…………………………………………………………………………………………………...68

LIST OF TABLES

Table **Page**

Table 1: Aspiration rate determination……………………………………………………...…..….20

Table 2: Determination of Nebulization Efficiency………….……………………….…….….….21

Table 3: Effect of Excess Sodium interference on Barium…………………………….……….24

Table 4: Effect of Excess Sodium interference on Cadmium…………………………….……..26

Table 5: Effect of Excess Sodium interference on Cobalt……….………………………..……..27

Table 6: Total analytes atoms reaching the Torch per concentration………………….….….…..32

Table 7: Total analytes atoms number density per concentration......................................…....34

Table 8: Calculation of the degree of ionization……………………………………..….….….37

Table 9: Degree of ionization per given concentration……………………..……….……..……39

Table 10: ∆E values of Theoretical Assumptions………………………………….……………41

Table 11: nµ'/nµ values when ∆E=0…………………………. …………….…….…….………42

Table 12: nµ'/nµ values when ∆E = IP (int) -IP (anal) …………………….…...……….........47

Table 13:nµ'/nµ values when∆E = kt -IP (anal……………………………………………………………………………53

ABBREVIATIONS

ICP	Inductively Coupled Plasma
ICP-OES	Inductively Coupled Plasma – OpticalEmission Spectroscopy
RF	Radio Frequency
PHZ	Pre-Heating Zone
IRZ	Initial Radiation Zone
NAZ	Normal Analytical Zone
ZWS	Zimbabwean Standard
CRM	Certified Reference Material
CCD	Charge Coupled Device
CID	Charge Injection Device

CHAPTER 1

1.0. INTRODUCTION

1.1 BACKGROUND

Zimbabwe's treated Municipal water has become scarce in most cities in the country, to such an extent that citizens have resorted to digging wells and boreholes to alleviate this problem. This well water is not subjected to thorough pre-treatment before consumption as compared to Municipal Water. Some have resorted to buying mineral water as the most trusted clean water, whose manufacturers have to meet Zimbabwe's food and drug regulations which requires the mineral water to be tested, certified and approved (ZW 560:1995). The standard requires that the total hardness in mineral water, which is usually as a resultant of the amount of Calcium and Magnesium be regulated. The amount of total hardness in a bottle of mineral water has to be regulated because excess consumption of the elements Ca and Mgwill lead to the development of gall stones, a medical condition which can affect digestion. Group II and Group I elements have proved to be common elements in the earth, undersea as well as in common water bodies. This widespread occurrence and the medical effect thereof, require an accurate analysis to quantify their concentration in mineral water before it gets on to the market. However the analysis of Calcium, Magnesium and subsequently Barium, Cadmium and Cobalt using the ICP-OES has a challenge of interferences in the presence of excess sodium and Potassium ions which are easily ionisable elements (Zaranyika MF,Chirenje AT, Mahamadi, 2007). This interference compromises the accurate quantification of the total hardness in mineral water either by decreasing or increasingthe intensities of the emission lines of the analyte.

1.2 STATEMENT OF THE PROBLEM

Inductively Coupled Plasma-Optical Emission Spectroscopy (ICP-OES) is the main method used to carry out analysis of the metal elements in drinking water and borehole water. This method can be affected by the interference effects of Group I elements particularly sodium and potassium such that some of the resultsobtained will either be enhanced or depressed. Barium, cobalt and cadmium quantification is a requisite before mineral water is registered here in Zimbabwe and SAZ has been using the ICP-OES instrument to quantify these elementswithout evaluating the levels at which the interference effects enhances signal detection or depression of the emission lines. The main issues of concern were the evaluation of the effect of excess sodium on barium, cobalt and cadmium emission signals.

1.3 OBJECTIVES

The objectives of this research is to

I) determine the interference effect (enhancement or depression) of sodium on Ba, Co and Cd

ii) Quantify the interference relationship between the analyte and the intereferent

iii) Model the interference effect of the easily ionisable elements on Barium, Cobalt and Cadmium

CHAPTER

2

2.0 LITERAURE REVIEW

2.1 Principles of Inductively Coupled Plasma – Optical Emission Spectroscopy.

Theseinstruments are classified according to the electrical field that is used to create the plasma (Hill, 2007) and these include

- Inductively Coupled Plasma (ICP) is obtained when a high-frequency field is applied through and around a coil
- Direct Current Plasma (DCP) is obtained when a direct current field is established and sustained across electrodes,
- Microwave-Induced Plasma (MIP) is obtained when a microwave field is applied to a cavity.

Fig:1 A typical inductively Coupled Plasma source.

Position A shows radial viewing of the torch, and position B shows axial viewing.The pioneer was the DCP plasma but as of now, the ICP is currently the most commonly used plasma. Originally, the ICP was designed for the production of crystals (Reed, 1961). The first analytical chemistry applications of the ICP were published in 1964 (Greenfield et al, 1964) and 1965 (Wendt and Fassel, 1965).Different names were used to describe the ICP and these included.

- induction-coupled plasma spectrometric excitation source (Wendt and Fassel, 1965)
- High frequency plasma source (Hoare and Mostyn, 1967) ,
- induction plasma (Biancifiori and Bordonali, 1967)
- induction-coupled, radio-frequency plasma torch (Veillonand Margoshes, 1968) ,

The gas used to generate the plasma is argon. It is a noble gas, which is a monoatomic element with a high ionization energy (15.76 eV), and is chemically inert.

2.1.1 Advantages of using Argon gas

- A simple spectrum is emitted by argon compared to a flame where molecularspectra are observed.
- Argon does not form stable compounds between itself and the analytes.
- However, some unstable molecular excited or ionized species can also be formed within the plasma (e.g. ArH) but they are usually dissociated after their excitation.
- Argon is also the cheapest noble gas.

2.1.2 Disadvantages of using argon

- It is a poor thermal conductor compared with other molecular gases for example nitrogen and hydrogen.

The high frequency field is produced by a radio frequency generator and accelerates argon electrons which later on ionize the plasma gas:

$$e + Ar \rightarrow Ar^{+} + e^{-} + e^{-}$$

The argon ions are recombined withelectrons to lead to excited argon atoms through a process known as radiative recombination which usually happens in the ultraviolet (UV) region

$$Ar^{+} + e^{-} \rightarrow Ar^{*} + h\,v$$

Except for the resonance lines that are located at 106.7 nm and 104.8 nm, there are no argon atomic lines below 300 nm.

In an Inductively coupled plasma optical emission spectrometry (ICP-OES), the source usually has two roles to play which are:

- atomization of the sample to be analysed into free analyte atoms in the ground state,
- Ionizationof the analyte atoms followed by excitation of the atoms and the ions to higher-energy states.

The plasma is the reservoir of energy provided by the radio frequency field, and it transfers this energy to an analyte.However, the atomization of a sample is a long process, whilst ionization and excitation are very fast processes. The major species are not only the argon ions, Ar+, and the electrons, e, but also the excited argon atoms, Ar*, with the special case of the metastable levels, Arm(Uchidaet al 1980).

2.2 Formation of ICP Plasma

The ICP is produced by passing initially ionized argon gas through a quartz torch embedded inside a Cu coil which is connected to a radio frequency (RF) generator (Montaser and Golightly, 1988). In most commercial units, the radio frequency generator provides up to 3 kW forward power at an approximate frequency of 27.1 MHzthesecurrents flowing in the Cu coil generate oscillating magnetic fields whose lines of force are axially oriented inside the quartz tube and follow elliptical closed paths outside the coil. Electrons and ions pass through the oscillating electromagnetic field flowing at high acceleration rates in closed annular paths inside the quartz tube space. The induced magnetic fields' direction and strength vary with time resulting in electron acceleration on each half cycle (Ingle and Crouch, 1988). Collisions between accelerated electrons, ions, and Ar gas cause further ionization. The collisions cause ohmic heating and, when measured spectroscopically, give thermal temperatures ranging from 6 000 to 10 000 K (Ingle and Crouch, 1988)

The quartz torch is made up of three concentric channels which are.

- The outer channel which conducts Ar gas at about 15 L min^{-1} to 17 L min^{-1} to sustain the plasma and induce the isolation of the quartz tube from high temperatures (Ingle and Crouch, 1988).
- The innermost channel which is meant for the introduction of a sample into the plasma.
- the middle channel which conducts the auxiliary argon gas at about 1 L min-1 and is mostly used when starting the plasma for organic samples analysis

The ICP has an annular, or donut, shape when viewed from above. Power dissipation is confined to the outer zones meaning that the axial zone in the centre has a relatively lower temperature than the outer donut body.

The cool centre forms a weak spot so that it is relatively easy to inject a gas stream (containing sample aerosol) through the centre without disturbing plasma stability. The sample is therefore heated from the outside by the surrounding plasma, and it goes through very high temperatures for relatively long periods of time, (Ingle and Crouch, 1988).

2.2.1 Zones of the Plasma

According to (Furuta, 1985), there is some confusion when dealing with the spatially resolved inter-elemental matrix effects regarding the criterion to indicate the exact plasma region that is being monitored.The central channel plasma is subsequently divided into three different zones which are;

- a pre-heating zone (PHZ)
- initial radiation zone(IRZ), in whichemission of atoms begin to be observed; and
- Normal analytical zone, (NAZ)the zone at which emission is produced mainly from ions (about 14 to 19 mm to the tip of the IRZ).

In the NAZ few inter-element effects exist (Furuta, 1985) (Ingle and Crouch, 1988). The IRZ extends upward to one or two mm above the load coil, adopting an amber bullet during the nebulization of many sample types containing calcium.

The IRZ is the plasma region where elemental matrix effect is strongest and must be avoided in analytical measurements (Zaranyika, 2000). In many cases, the variation of the matrix effect with radio frequency power and gas flow rate can be explained by a shift of the IRZ, because an increase in the gas flow rate and a decrease in radio frequency power move the IRZ up.

2.2.2 Configurations of the ICP Torch

There are two configurations which can be employed for observing emission from the ICP and these are:

- radial or side-on viewing of the plasma
- Axial or end-on viewing of the plasma.
- Dual view is the combination of these two basic modes.

2.2.2.1 Radial View and Axial View

The radial view is the classical operation mode for ICP-OES in which the plasma is operated ina vertical orientation, and the analytical zone is observed from the side of the plasma. Radial viewing constrains the observation volume in the NAZ, and thus limits the effect of potential spectral and background interferences (Hou and Bradley, 2000)

Fig 2 (i)the axial view

Fig 2 (ii) the radial view

With the axial view, the plasma is rotated to a horizontal position and the NAZ of the ICP is observed from the end of the plasma. The axial view provides better LODs than radial view(Lichte and Koirtyohann, 1976).This may be attributed to the longer viewing path available down the axis of the plasma. Thus, a better sensitivity and a 5- to 10- fold improvement in the LOD can be achieved.

2.2.2.2 Disadvantages of the axial view include:

- increased potential for spectral interference
- Increased potential for matrix-induced interferences.
- self-absorption effects because the observations are made through the much cooler tail plume of the plasma

These effects can besignificantly reduced by use of a shear gas which displaces the tail plume from the optical path thereby reducing the self-absorption(Demers, 1979). Spectral interferences may be either corrected or minimized by improving spectral resolution, using an alternate analytical line with less or no interference, or by applying an inter-element correction (IEC) factor.

In the event of using the axially viewed ICPs, the emissions from the excited analytes in the central column of the plasma are then isolated from the surrounding argon radiation (Brenner and Zander, 2000).Whilst focussing the spectrometer on the axial region through the transfer lenses or a flat mirror mounted above the vertically oriented plasma. A shear gas flow is then applied to remove the plasma fringe, minimize self-absorption, protect the optical interface from thermal damage, and above all prevent the salt deposits on the entrance optic lenses and mirrors to accumulate.

Fig 3: A shear gas blowing away possible salt deposits to the optical interface.

If the shear gas is N_2 or Ar it also allows for determinations in the UV region of the spectrum. The disadvantage of using air as a shear gas is the certainty of air entrainment(Brenner and Zander, 2000).

2.2.3 Dual View

In the analysis of very complicated sample matrices which have a wide range of elemental concentrations, the axial view is not very appropriate. Modern commercial instruments combine the axial view and radial view configurations into a single unit, which is known as the dual view (Hou and Jones, 2000).This dual view system allows the user to optimize the appropriate configuration for the type of sample without the expense of two separate ICP-OES systems(Boss and Fredeen1997),

2.2.4.1 Temperature and electron number density

The signal intensity observed when an element is analysed spectrochemically using the inductively coupled plasma optical emission spectroscopy, is a function of temperature and electronnumber density(Norwak, 1988). During the plasma initiation process,radio frequency power is coupled to the ICP by electron acceleration induced by the load coil.Ions pick up the radio frequency less efficiently compared to the electrons such that electronsgain the radio frequency energy in the induction zone and rapidly transfer it to ions and neutral ions. Because of the size of the collisional cross sectional area between electrons and ions, the ions gain energy from electrons much faster than atoms .Such that the electrons will be described by a temperature greater than ion temperature which will be greater than neutral atom temperature.

Different authors have evaluated and measured the electron number density and the temperature thereof.It has been realised that the values differ considerably. This is due to the spatial inhomogeneity of the plasma itself. A reliable electron number density can be determined in the ICP without any Local thermal equilibrium assumptions (Wendt, 1965).Different temperatures have also been defined for the ICP including the ionisation temperature, electron temperature, gastemperature and excitation temperature.

However, the electron temperature has to be measured.There are different types of methods used to measure this temperature and these are

- Saha Eggert ionisation equilibrium method
- Line merging at series limit
- Stark broadening of spectral lines

The Saha Eggert ionisation method has been used in this research and has proved to be quite accurate.

2.2.4.2 Local Thermodynamic Equilibrium

Local thermodynamic equilibrium is a situation existing in the plasma in which all the equilibrating processes in the system are due to collisional processes and all the radiative processes contribute to such a system a small degree to the total energy of the system such that they can be neglected. Within such a system,the populations of the energy levels within any ionisation stage can be calculated by the Boltzmann equation as follows.

$$\frac{n_2}{n_1} = \frac{g_2}{g_1}\ exp - (\frac{E_2 - E_1}{kT})$$

Whilst the relative ion level populations of two adjacent ionization stages can be calculated using the Saha equation as below

$$\frac{n_3}{n_1} = \frac{6.037x10^{21}}{n_e} . \frac{g_3}{g_1} . T_e^{3/2} . \exp\{-(\frac{E_3 - E_1}{kT})\}$$

Whilst the relative ion levels populations of two adjacent ionization stages can be calculated using the Saha equation as below

In which 1 and 2 are levels from some ionization stage (densities in cm^{-3}), and 3 is a level in some higher adjacent stage, g is the statistical weight, T_e is the electron temperature in in eV.E is the energy of a level (vs the ground atomic state value of zero) and n_e is the electron density.

2.2.4.3 Departures from Thermodynamic Equilibrium

Emissions in ICP-OES are produced by excited atoms or ions.This makes the process of excitation and ionisation of particular interest because the equilibrium based expressions do not correctly predict the experimentally measured emission intensities.The relative emission intensities and the extent of ionization would be easy to predict had the ICP been in thermal equilibrium. However, it is generally accepted that the inductively coupled plasma operated in argon is not in local thermodynamic equilibrium, at least in the region used for analytical observations between 5 and 30 mm above the radio frequency coil (Bowman, 1977).This summarises the results of the many various studies as follows

i) The observed concentrations of electrons and hence of argon ions ranging from 10^{14} cm^{-3} to $10cm^{-3}$ while explaining the absence of ionization interference in the argon ICP, cannot be reconciled with spectrochemically measured excitation temperatures using two line or many technique.

ii) The values found for such excitation temperatures increase with upper energy of transitions considered or in other words the relative overpopulation of an energy level increases with increasing excitation energy

iii) The intensity ratio of an ion line and an atom line of the same element is again significantly higher than expected from LTE expression using the obtained excitation temperature.

These observations may be expressed as follows

$T_{Ar\ ion}$ >Te>T_{ion}>T_{exc}> T_g

$T_{Ar\ ion}$ is the argon ionization temperature, T_e is the electron temperature. T_{ion} is the analyte ionization temperature, T_{exc} is the analyte excitation temperature and T_g is the gas or heavy particle temperature (Hanselman, 1994).

2.2.5 Ionisation interference

Group 1 elements are common in the matrix of environmental samples and products. The EIEs have been mostly studied in the field of elemental matrix effects in ICP-OES. This is due to several reasons, among them

- the historical tradition, since the effects of the these elements have been widely studied in flames (Forster,et al 1959))
- The effect of EIEs in ICPs is less pronounced than in flames and other types of plasmas such as the dc plasmas.
- the effects produced by EIEs are more pronounced than those observed for non EIEs;
- there are many samples containing high concentration of these elements; and

In spite of the huge volume of work reported, there is still no agreement on the dominant mechanism (Goldfarb, 1998)

However, it is not only the low IP elements that cause a matrix effect. Elements with a higher IP also have been shown to give rise to similar effects on the analytical signal. The effect of EIEs on plasma spectrochemical techniques is rather complex and “studying the literature on these interferences in the ICP has been termed a study of confusion” by Blades and Horlick (Blades et al 1981), who initially attributed this confusion to the inconsistency of the data that had appeared in the literature concerning these matrix effects.

This is because some workers had found enhancements, depressions or no effects at all on the analytical signal when EIEs were present. In addition, there is no satisfactory mechanistic account of how the interferences are produced. As noted by various authors, (Zaranyika and Makuhunga, 1997), the sources of EIEs interferences are not fully characterized such that there have been a number of publications on modelling of the effects of EIEs, in a field that has become to be known as plasma diagnostics. Plasma diagnostics is concerned with studying processes occurring within the plasma. Zaranyika and Mahamadi (2013) argued that according to the Local thermodynamics approach, the intensities of the atomic line absorption and the atomic line emission are directly proportional to the number of ground and excited states thus $A \propto n_0$ and $I \propto no$ in which I is the line emission signal intensity and A is the absorption signal intensity. These are related in the Boltzmann equation as follow

$$n_u = n_o . \left(\frac{g_u}{g_o} \right) \exp^{\left(\frac{-\Delta E}{KT} \right)}$$

In which

g_u and**g_o** are the statistical weights of the excited and the ground states

K is the Boltzmann constant

T is the absolute temperature

Δ**E** is the difference in the energies of the two electronic states involved in the transition.

2.2.6 Simplified reaction rate model

Zaranyika et al. (2000) have used simplified reaction rate models which focus on only one particular electronic level for the effect of EIEs in the air-acetylene flame. Along with the simplified models, they proposed a novel method for probing changes in the number density of the analyte excited state, n_u, based on determining the analyte emission (E) signal ratio and theintereferent$E^{'}$, where the prime denotes presence of interferent, and comparing to theoretical values derived assuming a simplified rate model based on steady state kinetics in the plasma for absorption. This hypothesis has also been tested through the use of the derived steady-state relationships and appropriate experimentally developed parameters for emission lines and their intensities.

CHAPTER

3

EXPERIMENTAL SECTION

3.0 Methodology

The experiments involved the analysis of emission line signals from the spiked samples (E') and the unspiked samples (E). The calculated ratios E'/E is then used for comparison.The effects of EIE was studied from two different angles and approaches in which the experimentally obtained E'/E values plotted against the concentration was compared with the theoretical perspective in which theoretically obtained values were also plotted against the concentration .A concentration rangeof 0-10mg/l was used on Cobalt and Cadmium whilst 0-28mg/l concentration range was used on Barium.

3.1 Equipment

Inductively coupled plasma Optical Emissions Spectroscopy (ICP-OES) was used for the experimental work. The instrument was supplied by ThermoFischer group. The instrument is an ICAP 6000 series.The type of the instrument is an ICAP 6500 radial (serial number ICP-20104501) with aradio frequency of 50/60 hertz. The high voltage of 200 – 240 volts exerts a high power of 4000VA (4kVA).This also enables the sample to"see" a higher plasma temperature, experience better excitation with less heat dissipation. ICAP 6500 has a radial and plasma view with a solid state RF generator ranging from 750 – 1600W.Argon gas control is made effective through a mass flow control with a 4 channel sample pump with a measurement mode which emphasises on speed and precision.It has additional techniques which include auto optimisation, auto sampler and room for transient accessories.The Argon gas was supplied by BOC Gases Zimbabwe which had a purity of 99.99%.The instrument was optimised using 40 ppm of Barium. The instrument has a detector which is totally enclosed within a window which is angled to reduce stray light.The detector is surrounded with a coolant system to avoid heating up and is connected to a processor.The CID detector has advantages over the CCD detector in that there is reduced pixel cross over,low noise effect, highly sensitive and reads the charge many times to reduce the read noise.

The instrument allows automated method development using the “optimise Source” routine. It automatically optimizes RF power, Nebuliser gas flow, Pump speed, Coolant gas flow, Auxiliary gas flow and the radial viewing.

3.2 MATERIALS

The following materials were used during the experiments and these include.

1.**Barium standard solution**: 993mg/kg ±5 with the following impurities in µg/ml, Mg<0.02, Pd<0.02, Re<0.02, S<0.02, Ni<0.02, Cu<0.02, Ba<0.02, Ce<0.02, W<0.02, Na <0.1, K<0.20, Cd<0.02,

2**. Cobalt standard solution**: 983mg/kg ±4 with the following impurities in µg/ml, Ga<0.02, He<0.02, Zn<0.02, Mg<0.02, Ba<0.02, B<0.05, Li<0.02, S<0.2,Fe <0.05, P <0.20, Se <0.2

3.**Cadmium standard solution**: with the following impurities in µg/ml Cu<0.02, Ba<0.02, Ce<0.02, W<0.02, Cd <0.02, Co <0.02, Zn<0.02, Mg<0.02, Ba<0.02, B<0.05

4. **SodiumChloride Analytical reagent:** Assay ≥99%, As ≤0.0002%, Pb ≤0.001, Fe≤0.001%, Mg ≤0.05%, K≤0.001%, Na≤0.02%

The deionised water used for the analysis had a an average conductivity 0.0034 micro Siemen

3.3 PROCEDURE

The procedure used for the experiment research was very similar to the one used by Zaranyika and co-workers. This procedure involved the preparation of two sets of standard solutions which however differed in range as follows, Cobalt 0-10mg/l , Barium 0 -28mg/l and Cadmium 0-10mg/l .All these standards were prepared from freshly prepared standard solutions.The first set was left unspiked whilst the second set was spiked with 1000mg/l of Sodium Chloride analytical grade reagent.The concentration of the different analytes was varied, whilst holding the high concentration of the sodium chloride interferent constant. This variation allowed for the analysis of the effect of the intereferent on the different concentrations of the analyte in relation to the instrument performance at high analyte concentrations and below.

3.4 Average Aspiration Rate Determination

The aspiration rate was determined by the use of two solutions a 0.2ppm and 5ppm standard solution which were spiked with 1000ppm sodium intereferent.Each sample was run 3 times in which the time taken for a particular volume of the sample analyte and the corresponding weight were taken into consideration.The average aspiration rate was determined for the different solutions which were also averaged to come up with an overall aspiration rate.

Table 1: Average Aspiration Rate Determination

Sample (ppm)	Aspiration Rate
0.2	2.600
0.2 + 1000mg Na	2.610
5	2.590
5 + 1000mg Na	2.632
Average	2.608±0.0179

3.5 Nebulisation Efficiency

The nebulisation efficiency determines the efficiency at which the analyte is converted into tiny drops which can then be sprayed into the torch.This determines the amount of analyte reaching the flame and subsequently the extent of analytes measurement.There are other attributes which also affect the nebulisation efficiency and these include the parameter setting made on the selected method from the instrument. The nebulisation gas flow rate has an impact on the nebulisation efficiency, so does the viscosity of the sample as well as the type of nebuliser that is fitted on to the instrument. For the ICAP 6500 instrument used, the nebulisation efficiency was determined by recording the mass of the total analyte aspirated into the instrument and the total mass of analyte collected from the residual tube. The difference between these two masses determined the analyte mass nebulised into the plasma.Four runs were done for the nebulisation efficiency using a 0.4ppm sample as follows

Table 2:Average Nebulisation Efficiency

Initial mass of Solution (g)	Mass of recovered solution (g)	Mass nebulised (g)	Nebulisation Efficiency as apercentage
9.7927	9.2289	0.5638	5.758
9.8823	9.3135	0.5688	5.756
9.8749	9.3062	0.5687	5.760
9.8579	9.2895	0.5684	5.766
		Mean	5.760 ±0.00432

The average nebulisation efficiency for the ICP-OES instrument was 5.760%

3.6 Determination of plasm temperature

A sample of Cadmium was prepared from the standard solutions and spiked with 1000ppm sodium. It was then measured at two different wavelengths which are whilst recording the emission intensities. These values were then used to determine the change in energies ΔE at the different wavelengths and used to calculate the temperature by making T the subject of the formulae in the following equation.

$$\frac{nu_1}{nu_2} = \frac{gu_1}{gu_2} e^{\left(\frac{-\Delta E_1}{KT}\right) + \left(\frac{\Delta E_2}{KT}\right)}$$

In which

gu and go are the statistical weights of the excited and the ground states

K is the Boltzmann constant

T is the absolute temperature

ΔE is the difference in the energies of the two electronic states involved in the transition

Wavelength 1 = 228.616		g_1=11	Wavelength 2 = 238.892	
Intensity	= 2265	g_2=13	Intensity	=2316

K= 1.38064×10^{-23}

ΔE_1 = hc/λ = $(6.63 \times 10^{-34} \times 2.99792458 \times 10^{8}) / (228.616 \times 10^{-7})$

= $8.694159624 \times 10^{-21}$

ΔE_2 = hc/λ = $(6.63 \times 10^{-34} \times 2.99792458 \times 10^{8}) / (238.892 \times 10^{-7})$

= $8.320178141 \times 10^{-21}$

$$\frac{2265}{2316} = \frac{11}{13} e^{\frac{-(8.694159624\, x\, 10^{-21}}{T1.38064E-23} \quad + \quad \frac{8.320178141\, x\, 10^{-21})}{T1.38064XE-23}}$$

$$0.977979274 \text{ X } (13/11) = e^{\frac{1.701433777 \, x \, 10^{-20}}{T 1.38064 \, X 10^{-23}}}$$

$$1.155793687 = e^{\frac{1232.351501}{T}}$$

$$\text{In } 1.155793687 = \frac{1232.351501}{T}$$

$$\text{T In } 1.155793687 = 1232.351501$$

$$T = \frac{1232.35150}{In \; 1.155793687}$$

$$T \quad \mathbf{= -8511.46K}$$

CHAPTER

4

4.0 THEORETICAL AND EXPERIMENTAL CALCULATIONS

4.1 Experimental Result

Table 3:Effect of Excess Sodium Intereferent on Barium

Concentration	E	E’	E’/E
1	125220	90770	0.724884204
2	182220	168220	0.923169795
3	303220	270420	0.891827716
4	402720	309020	0.767332141
5	479720	469220	0.978112232
6	575220	442920	0.770001043
7	662020	633920	0.957554152
8	748620	709520	0.947770565
9	862320	792120	0.918591706
10	931320	860420	0.923871494
11	1029520	961820	0.9342412
12	1090520	1015520	0.93122547
13	1162520	1128520	0.970753191
14	1264520	1177520	0.93119919
15	1387520	1235520	0.89045203
16	1411520	1318520	0.93411358
17	1567520	1568520	1.00063795
18	1612520	1525520	0.946047181

19	1677520	1645520	0.980924221
20	1744520	1650520	0.946116983
21	1826520	1744520	0.955105884
22	1938520	1765520	0.91075666
23	2039520	1961520	0.961755707
24	2106520	2147520	1.01946338
25	2158520	2035520	0.943016511
26	2339520	2250520	0.961958008
27	2463520	2263520	0.918815354
28	2463520	2559520	1.03896863

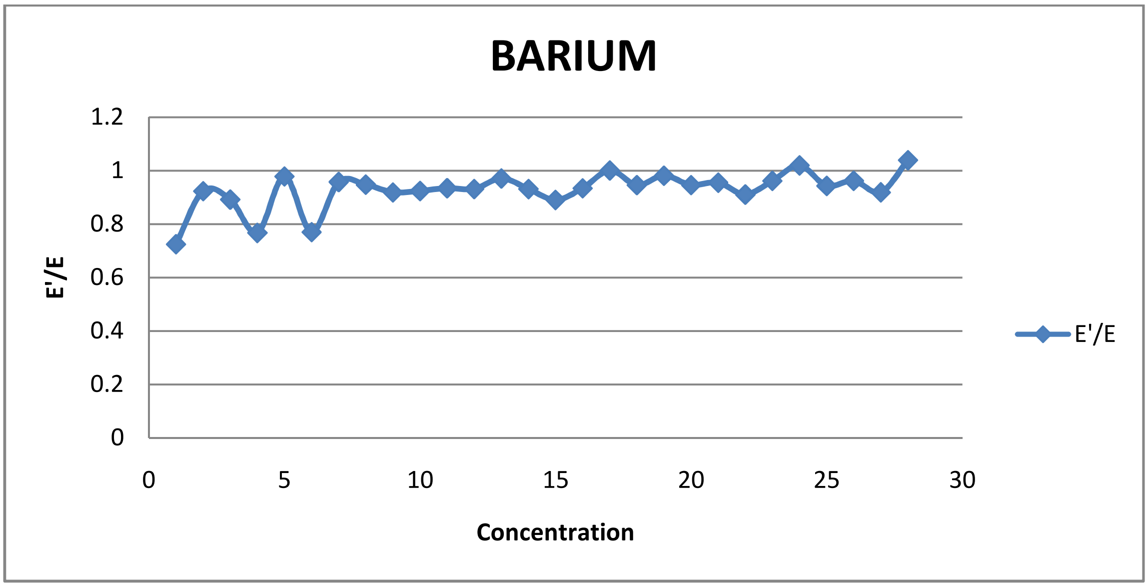

Fig 4: E’/E of Barium experimental interference with Sodium

Table 4: Effect of Excess Sodium intereferent on Cadmium

Concentration	E	E’	E’/E
0.1	210.5968	216.9968	1.030389825
0.2	211.7968	230.2968	1.087347873
0.3	240.9968	254.5968	1.056432285
0.4	249.2968	274.2968	1.100282073
0.6	288.8968	295.3968	1.022499384
0.8	328.8968	342.8968	1.042566544
1	401.6968	412.6968	1.027383838
2	542.4968	551.4968	1.01658996
3	976.3968	1006.997	1.031339718
4	1259.997	1408.997	1.118254269
5	1588.997	1780.997	1.120830954
6	1508.816	1211.666	0.803057497
7	1705.216	2500.226	1.466222461
8	1573.116	1880.936	1.195675335
9	2398.686	2608.116	1.087310302
10	2731.516	2922.246	1.069825694

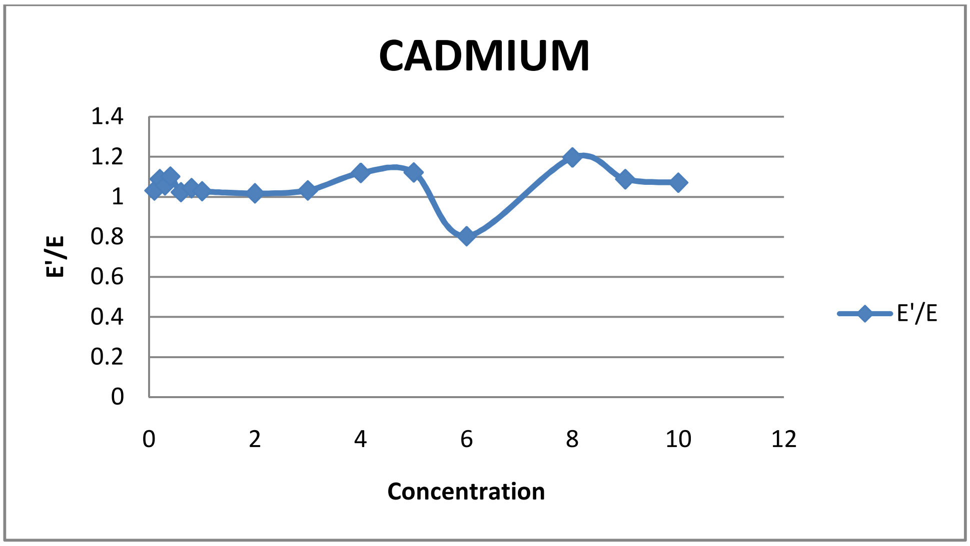

Fig 5: E'/E of Cadmium experimental interference with Sodium

Table 5:Effect of excess Sodium interference on Cobalt

Concentration	E	E'	E'/E
0.4	7.416	13.17	1.775889968
0.8	209.9529	268.7879	1.280229513
1	104.0299	127.3439	1.224108637
2	207.7289	221.2729	1.065200363
3	311.5079	315.5369	1.012933861
4	411.6549	423.7959	1.02949315
5	500.7419	510.5639	1.019614895
6	523.737	542.213	1.053285343
7	598.368	613.14	1.079089119
8	629.371	656.755	1.043510108

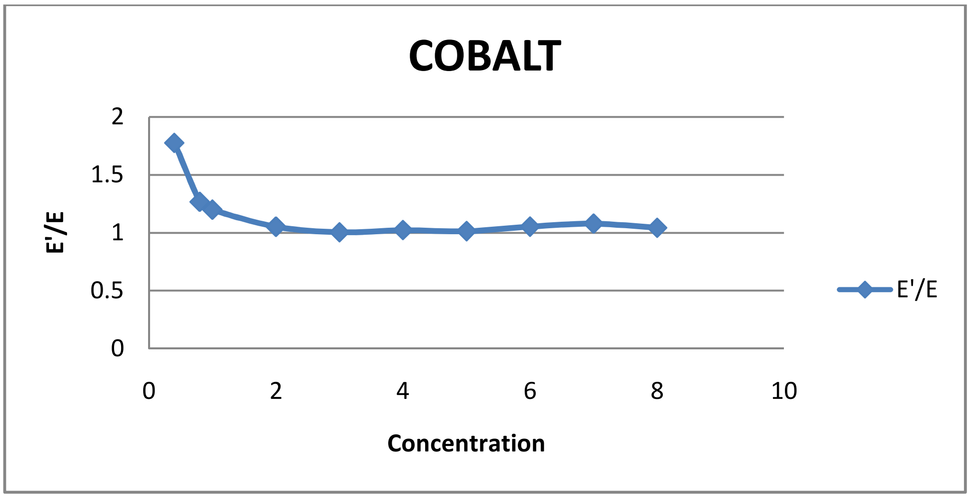

Fig 6: E’/E of Cobalt experimental interference with Sodium

4.2 THEORETICAL RESULTS

Interference of Co,Ba,and Cd with Na calculations

The total gaseous flow rate in the plasma torch is calculated by summing up the total sample flow rate and the total argon gas flow rate.The total gaseous flow rate is given by the following equation

$$\left(\frac{xf}{MW}\right)pX(22.4)X\left(\frac{T}{298}\right)X\left(\frac{1000}{60}\right)+\left(\frac{At}{298}\right)X\left(\frac{1000}{60}\right)$$

Aspiration Rate	x	2.608
Specific gravity	p	1
Nebulisation efficiency	f	0.0576
Temperature	T	8511.46
Molecular Weight	MW	18
Auxilliary Flow Rate	A	0.5

TOTAL GASEOUS FLOW RATE = SAMPLE SOLUTION FLOW RATE + ARGONAUXILLIARY FLOW RATE

= (xf)/MW (22.4) (8511.46/298) (1000/60) +[(At)/298] (1000/60)

= 88.99018954 +238.0162192

= **3.2700641X 10^2**

4.2.1 TOTAL ANALYTE ATOMS REACHING THE TORCH

For every sample measured, an aspirant of the argon gas and the sample flows into the plasma torch. However, not all the analytes atoms reach the torch for measurement. Hence the total analyte reaching the torch is calculated using the following formulae

$$nT = 1.0037 X 10^{16} X ([M] X 2.608 X 0.0576) XAW$$

In which

[M] = for the analyte concentration

AW= atomic weight

nT = total analyte atoms reaching the torch

Aspiration Rate=2.608

Constant = 1.0037E+16

Nebulisation efficiency = 0.0576

Table 6:Total Analyte atoms reaching the Torch per concentration

Analyte Concentration	***AW***	**0.1**	**0.2**	**0.3**	**0.4**	**0.6**	**0.8**	**1**	**2**	**3**	**4**
Cobalt	58.9332	2.56E+12	5.12E+12	7.68E+12	1.02E+13	1.54E+13	2.05E+13	2.56E+13	5.12E+13	7.68E+13	1.02E+14
Barium	56	2.69244E+12	5.38488E+12	8.07732E+12	1.07698E+13	1.61546E+13	2.154E+13	2.69E+13	5.38488E+13	8.07732E+13	1.08E+14
Cadmium	48	3.14118E+12	6.28236E+12	9.42354E+12	1.25647E+13	1.88471E+13	2.5129E+13	3.14E+13	6.28236E+13	9.42354E+13	1.26E+14

5	**6**	**7**	**8**	**9**	**10**	**11**	**12**	**13**	**14**	**15**	**16**	**17**

1.28E+14	1.54E+14	1.79E+14	2.05E+14	2.30E+14	2.56E+14	2.81E+14	3.07E+14	3.33E+14	3.58E+14	3.84E+14	4.09E+14	4.35E+14
1.35E+14	1.62E+14	1.88E+14	2.15E+14	2.42E+14	2.69E+14	2.96E+14	3.23E+14	3.5E+14	3.77E+14	4.04E+14	4.31E+14	4.58E+14
1.57E+14	1.88E+14	2.2E+14	2.51E+14	2.83E+14	3.14E+14	3.46E+14	3.77E+14	4.08E+14	4.4E+14	4.71E+14	5.03E+14	5.34E+14

18	**19**	**20**	**21**	**22**	**23**	**24**	**25**	**26**	**27**	**28**	**29**	**30**
4.61E+14	4.86E+14	5.12E+14	5.37E+14	5.63E+14	5.88E+14	6.14E+14	6.4E+14	6.65E+14	6.91E+14	7.16E+14	7.42E+14	7.68E+14
4.85E+14	5.12E+14	5.38E+14	5.65E+14	5.92E+14	6.19E+14	6.46E+14	6.73E+14	7E+14	7.27E+14	7.54E+14	7.81E+14	8.08E+14
5.65E+14	5.97E+14	6.28E+14	6.6E+14	6.91E+14	7.22E+14	7.54E+14	7.85E+14	8.17E+14	8.48E+14	8.8E+14	9.11E+14	9.42E+14

4.2.2 ANALYTE NUMBER DENSITY

The analyte number density is calculated by considering the relationship between the total analyte reaching the torch (which is a function of the concentration and the molecular weight) and the flow rate at which the aspirant will be flowing. This relationship establishes the amount of analyte per given volume of aspirant within a specific concentration. Given that the total gaseous flow rate into the torch is 3.2700641 X 10^2, the analyte number densities per concentration is given below

Table 7: Total analyte number density per concentration (ppm)

Analyte Concentration	**AW**	**0.1**	**0.2**	**0.3**	**0.4**	**0.6**	**0.8**	**1**	**2**	**3**	**4**
Cobalt	58.9332	7.82E+09	1.56E+10	2.35E+10	3.13E+10	46942796257	6.259E+10	7.82E+10	1.56476E+11	2.34714E+11	3.13E+11
Barium	56	8.23E+09	1.65E+10	2.47E+10	3.29E+10	49401592864	6.5869E+10	8.23E+10	1.64672E+11	2.47008E+11	3.29E+11
Cadmium	48	9.61E+09	1.92E+10	2.88E+10	3.84E+10	57635191675	7.6847E+10	9.61E+10	1.92117E+11	2.88176E+11	3.84E+11

5	**6**	**7**	**8**	**9**	**10**	**11**	**12**	**13**	**14**	**15**	**16**	**17**
3.91E+11	4.69E+11	5.48E+11	6.26E+11	7.04E+11	7.82E+11	8.61E+11	9.39E+11	1.02E+12	1.1E+12	1.17E+12	1.25E+12	1.33E+12
4.12	4.94	5.76	6.59	7.41	8.23	9.06	9.88	1.07	1.15	1.24	1.32	1.4E

E+11	E+11	E+11	E+11	E+11	E+11	E+11	E+11	E+12	E+12	E+12	E+12	+12
4.8E+11	5.76E+11	6.72E+11	7.68E+11	8.65E+11	9.61E+11	1.06E+12	1.15E+12	1.25E+12	1.34E+12	1.44E+12	1.54E+12	1.63E+12

18	**19**	**20**	**21**	**22**	**23**	**24**	**25**	**26**	**27**	**28**	**29**	**30**
1.41E+12	1.49E+12	1.56E+12	1.64E+12	1.72E+12	1.8E+12	1.88E+12	1.96E+12	2.03E+12	2.11E+12	2.19E+12	2.27E+12	2.35E+12
1.48E+12	1.56E+12	1.65E+12	1.73E+12	1.81E+12	1.89E+12	1.98E+12	2.06E+12	2.14E+12	2.22E+12	2.31E+12	2.39E+12	2.47E+12
1.73E+12	1.83E+12	1.92E+12	2.02E+12	2.11E+12	2.21E+12	2.31E+12	2.4E+12	2.5E+12	2.59E+12	2.69E+12	2.79E+12	2.88E+12

4.2.3 DEGREES OF IONISATION USING THE SAHA EQUATION

The degree of ionisation is calculated using the Saha equation as follows

$$\log\left(\frac{N_+ N_e}{N}\right) = x\Phi - \frac{3}{2} + \log\Phi + 20.9366 + \log\left(\frac{2U_+}{U_o}\right)$$

In which x = ionization potential

φ = 5040 / T

U = partition function

N = number density and the subscripts 0, + and e denote the ground state, ion and electron respectively

Table 8: Calculation of the N_+N_e/N_o

DEGREES OF IONISATION USING THE SAHA EQUATION				log (N+Ne/No) =	xθ-3/2*logθ+20.9366+Log(2U+/Uo)	
EQUATION		log U+	Log Uo	Log(2U+/Uo)	3/2*logθ	k
ELEMENT		U+ =42.65795188	Uo=53.76317964		θ=5040/8511.46 =0.592142411	
Cobalt		1.63	1.73	0.201029996	-0.341360749	20.936
Barium		0.85	0.92	0.231029996	-0.341360749	20.936
Cadmium		0.3	0.02	0.581029996	-0.341360749	20.936

Conc	**0.1**	**0.2**	**0.3**	**0.4**	**0.6**	**0.8**	**1**	**2**	**3**	**4**
ELEMENT	**N_t/Ne**									
Cobalt	2.25354E+13	3.18699E+13	3.90325E+13	4.50708E+13	5.52002E+13	6.374E+13	7.13E+13	1.00781E+14	1.23431E+14	1.43E+14
Barium	6.72813E+13	9.51501E+13	1.16535E+14	1.34563E+14	1.64805E+14	1.903E+14	2.13E+14	3.00891E+14	3.68515E+14	4.26E+14

Cadmium	2.60973E+13	3.69072E+13	4.52019E+13	5.21946E+13	6.39251E+13	7.3814E+13	8.25E+13	1.16711E+14	1.42941E+14	1.65E+14

5	**6**	**7**	**8**	**9**	**10**	**11**	**12**	**13**	**14**	**15**	**16**	**17**
1.59E+14	1.75E+14	1.89E+14	2.02E+14	2.14E+14	2.25E+14	2.36E+14	2.47E+14	2.57E+14	2.67E+14	2.76E+14	2.85E+14	2.94E+14
4.76E+14	5.21E+14	5.63E+14	6.02E+14	6.38E+14	6.73E+14	7.06E+14	7.37E+14	7.67E+14	7.96E+14	8.24E+14	8.51E+14	8.77E+14
1.85E+14	2.02E+14	2.18E+14	2.33E+14	2.48E+14	2.61E+14	2.74E+14	2.86E+14	2.98E+14	3.09E+14	3.2E+14	3.3E+14	3.4E+14

18	**19**	**20**	**21**	**22**	**23**	**24**	**25**	**26**	**27**	**28**	**29**	**30**
3.02E+14	3.11E+14	3.19E+14	3.27E+14	3.34E+14	3.42E+14	3.49E+14	3.56E+14	3.63E+14	3.7E+14	3.77E+14	3.84E+14	3.9E+14
9.03E+14	9.27E+14	9.52E+14	9.75E+14	9.98E+14	1.02E+15	1.04E+15	1.06E+15	1.08E+15	1.11E+15	1.13E+15	1.15E+15	1.17E+15
3.5E+14	3.6E+14	3.69E+1	3.78E+1	3.87E+1	3.96E+1	4.04E+1	4.13E+1	4.21E+1	4.29E+1	4.37E+1	4.44E+1	4.52E+1

		4	4	4	4	4	4	4	4	4	4	4

Table 9: Calculation of the degree of Ionisation per concentration (ppm)

Element	**0.1**	**0.2**	**0.3**	**0.4**	**0.6**	**0.8**	**1**	**2**	**3**	**4**
Cobalt	288036.5636	203672.6073	166297.9875	144018.2818	117590.4347	101836.304	91085.16	64406.93362	52588.04109	45542.58
Barium	817154.8396	577815.7284	471784.5666	408577.4198	333602.0663	288907.864	258407	182721.377	149191.3795	129203.5
Cadmium	271680.9328	192107.4299	156855.0597	135840.4664	110913.2764	96053.7149	85913.05	60749.70339	49601.92511	42956.53

5	**6**	**7**	**8**	**9**	**10**	**11**	**12**	**13**	**14**	**15**	**16**	**17**
40734.52	37185.36	34426.95	32203.47	30361.72	28803.66	27463.21	26294.02	25262.48	24343.53	23518.09	22771.29	22091.4
115563.1	105494.2	97668.68	91360.69	86135.68	81715.48	77912.66	74595.69	71669.22	69062.19	66720.41	64601.76	62672.92

38421.49	35073.86	32472.08	30374.85	28637.68	27168.09	25903.76	24800.96	23827.99	22961.23	22182.66	21478.26	20836.98

18	**19**	**20**	**21**	**22**	**23**	**24**	**25**	**26**	**27**	**28**	**29**	**30**
21468.98	20896.37	20367.26	19876.41	19419.42	18992.57	18592.68	18217.03	17863.27	17529.35	17213.48	16914.09	16629.8
60907.13	59282.64	57781.57	56389.04	55092.57	53881.59	52747.12	51681.41	50677.79	49730.46	48834.34	47984.98	47178.46
20249.9	19709.81	19210.74	18747.77	18316.72	17914.11	17536.93	17182.61	16848.94	16533.98	16236.04	15953.65	15685.51

4.3 GRAPHICAL PRESENTATION

Three scenarios were investigated and the theoretically plotted graphs were then simulated to see the closeness of fit with the experimentally obtained graphs. These scenarios were simulated under the following assumptions

- ΔE = 0 :Assumes that there is no change in the populations of theground and excited states of analyte atoms E'/E=1
- ΔE = IP (int) - IP (anal) Assumes that there is an increase of ground state, for example the suppression of ionization: E'/E>1
- ΔE = kt -IP (anal) Assumes that there is depopulation of the ground state, for example through charge transfer reactions E'/E< 1

Table 10: ΔE values of theoretical assumptions

	Ionisation Potential	**K**	**T**	**ΔE = 0**	**ΔE = IP (int) - IP (anal)**	**ΔE = kt -IP (anal)**
Cobalt	7.881	1.38064 X 10^{-23}	8511.46	0	-2.7419	-7.881
Barium	5.2117	1.38064 X 10^{-23}	8511.46	0	-0.0726	-5.2117
Cadmium	8.9938	1.38064 X 10^{-23}	8511.46	0	-3.8547	-8.9938
Na Intereferent	5.1391					

4.3.1 When ΔE =0

Substituting the values of ΔE into the following equationand potting the values of ηύ/ημ against the concentration

$$\frac{n\mu'}{n\mu} = 1 + \frac{ne'}{no}\ X\ e^{\left(\frac{\Delta E}{KT}\right)}$$

Table 11: ηύ/ημ values when ΔE=0

	0.1	**0.2**	**0.3**	**0.4**	**0.6**	**0.8**	**1**	**2**	**3**	**4**	**5**
Cobalt	9.874924544	7.275519328	6.123940075	5.437462272	4.623172773	4.13775966	3.806498	2.984493458	2.620332123	2.403249	2.255104
Barium	3.972596326	3.10194302	2.716229289	2.486298163	2.213557368	2.05097151	1.940017	1.664692745	1.542719354	1.470009	1.420389

Cadmium	8.663626749	6.419002442	5.424596966	4.831813374	4.128662519	3.70950122	3.423452	2.713639036	2.399180414	2.211726	2.0838

5	**6**	**7**	**8**	**9**	**10**	**11**	**12**	**13**	**14**	**15**	**16**	**17**
2.255104	2.145748	2.060756	1.992247	1.935499	1.887492	1.846191	1.810166	1.778382	1.750068	1.724635	1.701624	1.680676
1.420389	1.383761	1.355293	1.332346	1.313339	1.29726	1.283426	1.27136	1.260714	1.25123	1.242711	1.235004	1.227988
2.0838	1.98937	1.915979	1.85682	1.807817	1.766363	1.730698	1.69959	1.672145	1.647695	1.625733	1.605863	1.587773

18	**19**	**20**	**21**	**22**	**23**	**24**	**25**	**26**	**27**	**28**	**29**	**30**
1.661498	1.643855	1.627552	1.612428	1.598347	1.585195	1.572874	1.5613	1.550399	1.540111	1.530378	1.521154	1.512394
1.221564	1.215655	1.210194	1.205129	1.200412	1.196007	1.19188	1.188003	1.184353	1.180906	1.177647	1.174557	1.171623
1.571213	1.555978	1.5419	1.52884	1.516682	1.505325	1.494685	1.48469	1.475278	1.466393	1.457989	1.450024	1.44246

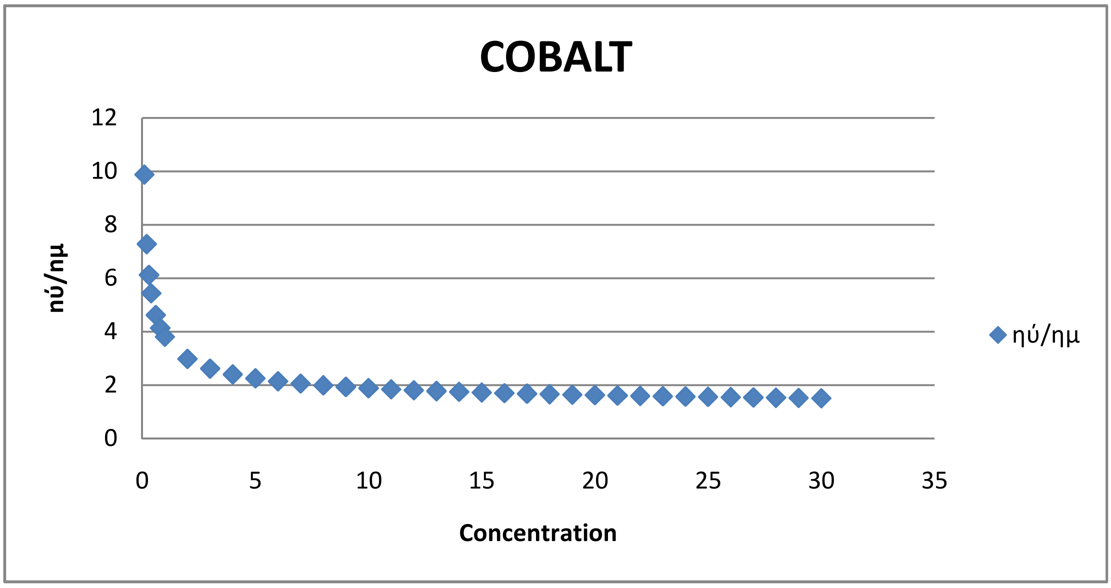

Fig 7 :ηύ/ημof Cobalt Theoreticall interference with Sodium when ΔE=0

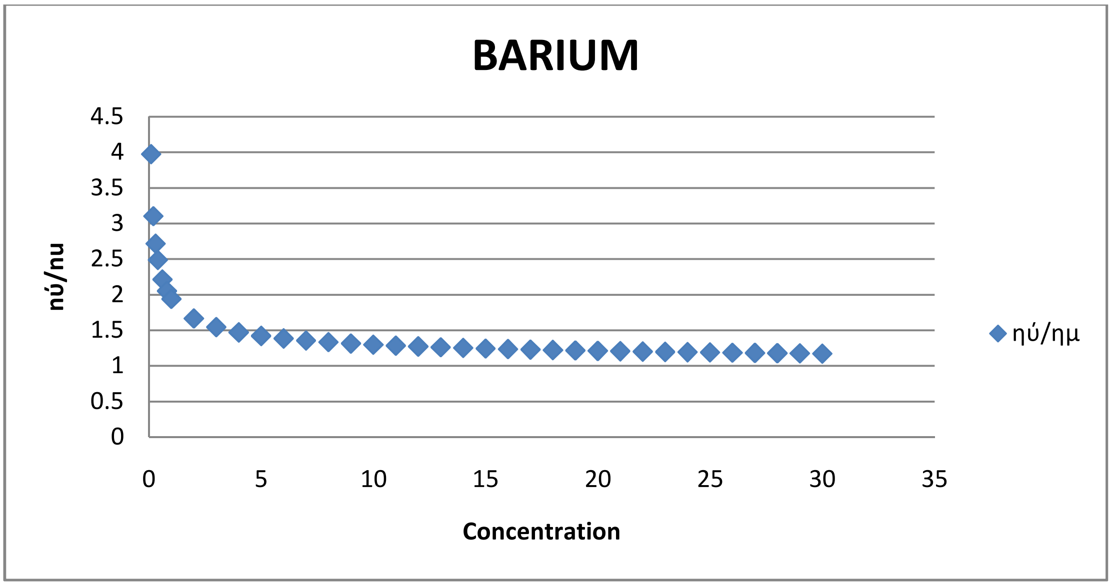

Fig 8: ηύ/ημ of Barium Theoreticall interference with Sodium when ΔE=0

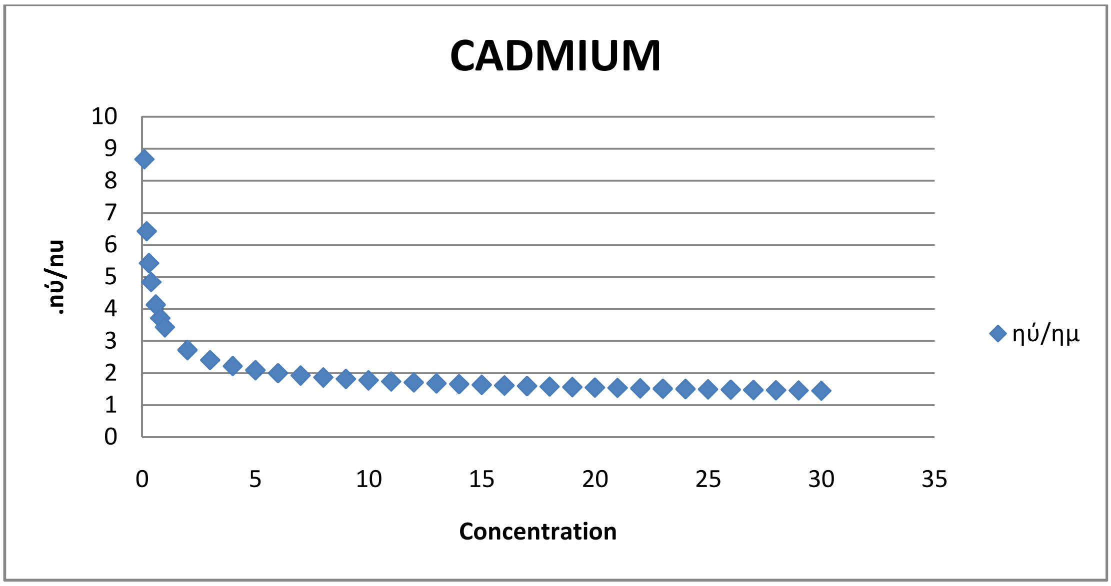

Fig 9:ηύ/ημ of Cadmium Theoreticalinterference with Sodium when ΔE=0

4.3.2When ΔE = IP (int) -IP (anal)

Substituting the values of ΔE into the following equationand potting the values of ηύ/ημ against the concentration

$$\frac{n\mu'}{n\mu} = 1 + \frac{ne'}{no}\ X\ e^{(\frac{\Delta E}{KT})}$$

Table 12: ηύ/ημ when ΔE = IP (int) - IP (anal)

conc		0.1	0.2	0.3	0.4	0.6	0.8	1	2	3	4

Cobalt	ηe'/ηo	8.874924544	6.275519328	5.123940075	4.437462272	3.623172773	3.13775966	2.806498	1.984493458	1.620332123	1.403249
ηύ/ημ		1	1	1	1	1	1	1	1	1	1
Barium	ηe'/ηo	2.972596326	2.10194302	1.716229289	1.486298163	1.213557368	1.05097151	0.940017	0.664692745	0.542719354	0.470009
ηύ/ημ		1	1	1	1	1	1	1	1	1	1
Cadmium	ηe'/ηo	7.663626749	5.419002442	4.424596966	3.831813374	3.128662519	2.70950122	2.423452	1.713639036	1.399180414	1.211726
ηύ/ημ		1	1	1	1	1	1	1	1	1	1

5	**6**	**7**	**8**	**9**	**10**	**11**	**12**	**13**	**14**	**15**	**16**	**17**
1.255104	1.145748	1.060756	0.992247	0.935499	0.887492	0.846191	0.810166	0.778382	0.750068	0.724635	0.701624	0.680676
1	1	1	1	1	1	1	1	1	1	1	1	1
0.420389	0.383761	0.355293	0.332346	0.313339	0.29726	0.283426	0.27136	0.260714	0.25123	0.242711	0.235004	0.227988
1	1	1	1	1	1	1	1	1	1	1	1	1
1.08	0.98	0.91	0.85	0.80	0.76	0.73	0.69	0.67	0.64	0.62	0.60	0.58

38	937	5979	682	7817	6363	0698	959	2145	7695	5733	5863	7773
1	1	1	1	1	1	1	1	1	1	1	1	1

18	**19**	**20**	**21**	**22**	**23**	**24**	**25**	**26**	**27**	**28**	**29**	**30**
0.66 1498	0.64 3855	0.62 7552	0.61 2428	0.59 8347	0.58 5195	0.57 2874	0.56 13	0.55 0399	0.54 0111	0.53 0378	0.52 1154	0.51 2394
1	1	1	1	1	1	1	1	1	1	1	1	1
0.22 1564	0.21 5655	0.21 0194	0.20 5129	0.20 0412	0.19 6007	0.19 188	0.18 8003	0.18 4353	0.18 0906	0.17 7647	0.17 4557	0.17 1623
1	1	1	1	1	1	1	1	1	1	1	1	1
0.57 1213	0.55 5978	0.54 19	0.52 884	0.51 6682	0.50 5325	0.49 4685	0.48 469	0.47 5278	0.46 6393	0.45 7989	0.45 0024	0.44 246
1	1	1	1	1	1	1	1	1	1	1	1	1

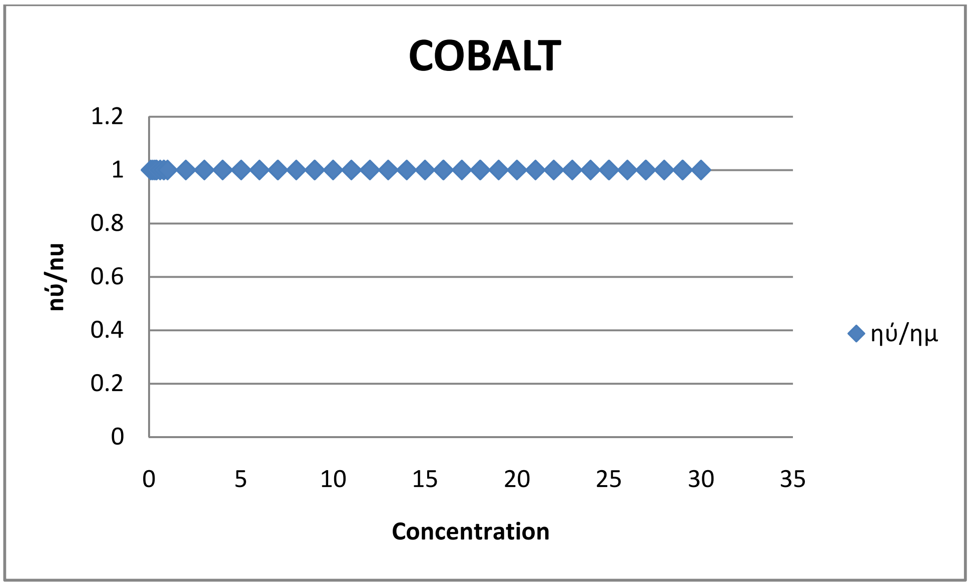

Fig 10: ηύ/ημ of Cobalt Theoretical interference with Sodium when ΔE = IP (int) -IP (anal)

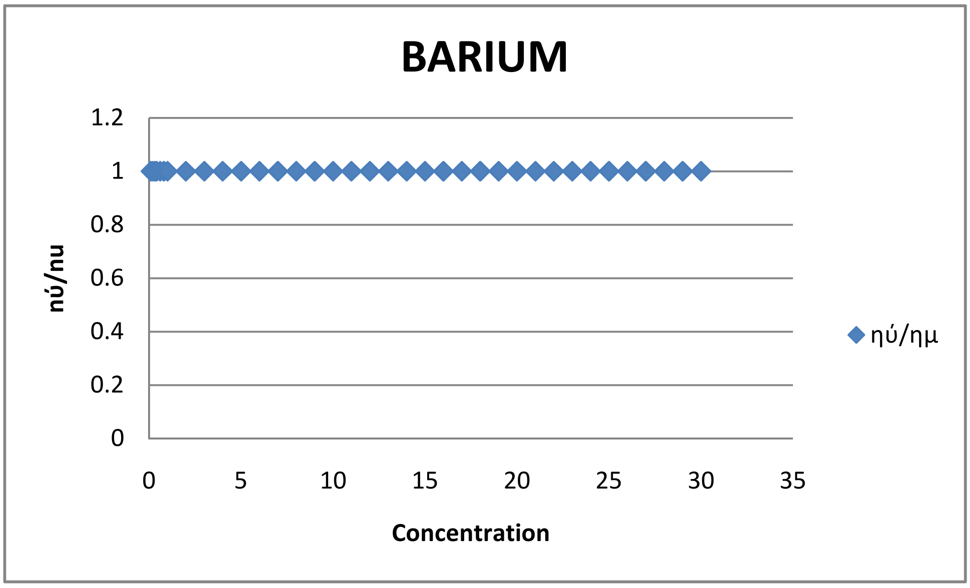

Fig 11: ηύ/ημ of Barium Theoretical interference with Sodium when ΔE = IP (int) -IP (anal)

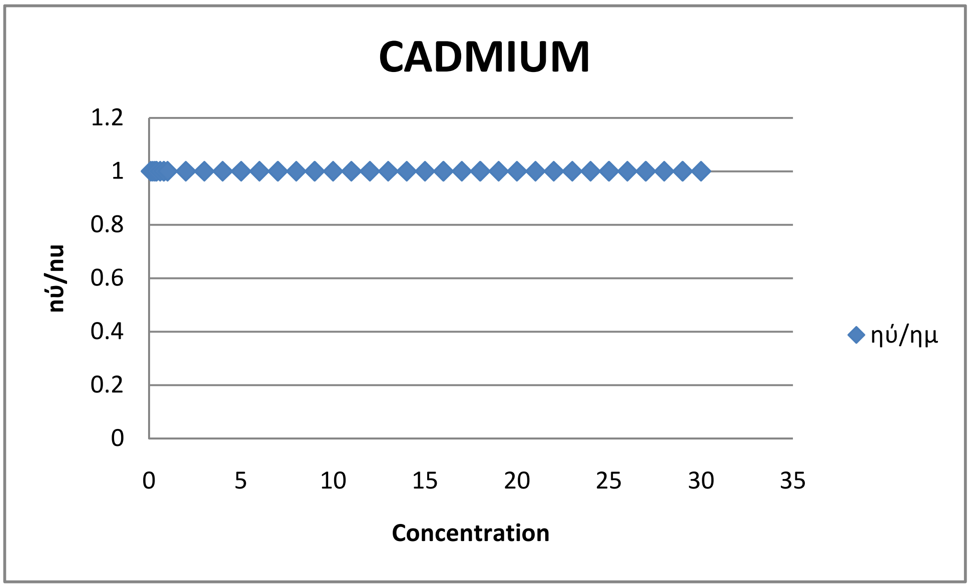

Fig 12: ηύ/ημ of Cadmium Theoretical interference with Sodium when ΔE = IP (int) -IP (anal)

4.3.3ΔE = kt -IP (anal)

Substituting the values of ΔE into the following equationand potting the values of ηύ/ημ against the concentration

$$\frac{n\mu'}{n\mu} = 1 + \frac{ne'}{no}\ X\ e^{(\frac{\Delta E}{KT})}$$

Table 13: ηύ/ημ when ΔE = IP (int) - IP (anal)

Conc		**0.1**	**0.2**	**0.3**	**0.4**	**0.6**	**0.8**	**1**	**2**	**3**	**4**
Cobalt	ηe'/ηo	8.874924544	6.275519328	5.123940075	4.437462272	3.623172773	3.13775966	2.806498	1.984493458	1.620332123	1.403249
ηύ/ημ		1	1	1	1	1	1	1	1	1	1
Barium	ηe'/ηo	2.972596326	2.10194302	1.716229289	1.486298163	1.213557368	1.05097151	0.940017	0.664692745	0.542719354	0.470009
ηύ/ημ		1	1	1	1	1	1	1	1	1	1
Cadmium	ηe'/ηo	7.663626749	5.419002442	4.424596966	3.831813374	3.128662519	2.70950122	2.423452	1.713639036	1.399180414	1.211726
ηύ/ημ		1	1	1	1	1	1	1	1	1	1

5	**6**	**7**	**8**	**9**	**10**	**11**	**12**	**13**	**14**	**15**	**16**	**17**
1.255104	1.145748	1.060756	0.992247	0.935499	0.887492	0.846191	0.810166	0.778382	0.750068	0.724635	0.701624	0.680676
1	1	1	1	1	1	1	1	1	1	1	1	1
0.42	0.38	0.35	0.33	0.31	0.29	0.28	0.27	0.26	0.25	0.24	0.23	0.22

0389	3761	5293	2346	3339	726	3426	136	0714	123	2711	5004	7988
1	1	1	1	1	1	1	1	1	1	1	1	1
1.08 38	0.98 937	0.91 5979	0.85 682	0.80 7817	0.76 6363	0.73 0698	0.69 959	0.67 2145	0.64 7695	0.62 5733	0.60 5863	0.58 7773
1	1	1	1	1	1	1	1	1	1	1	1	1

18	**19**	**20**	**21**	**22**	**23**	**24**	**25**	**26**	**27**	**28**	**29**	**30**
0.66 1498	0.64 3855	0.62 7552	0.61 2428	0.59 8347	0.58 5195	0.57 2874	0.56 13	0.55 0399	0.54 0111	0.53 0378	0.52 1154	0.51 2394
1	1	1	1	1	1	1	1	1	1	1	1	1
0.22 1564	0.21 5655	0.21 0194	0.20 5129	0.20 0412	0.19 6007	0.19 188	0.18 8003	0.18 4353	0.18 0906	0.17 7647	0.17 4557	0.17 1623
1	1	1	1	1	1	1	1	1	1	1	1	1
0.57 1213	0.55 5978	0.54 19	0.52 884	0.51 6682	0.50 5325	0.49 4685	0.48 469	0.47 5278	0.46 6393	0.45 7989	0.45 0024	0.44 246
1	1	1	1	1	1	1	1	1	1	1	1	1

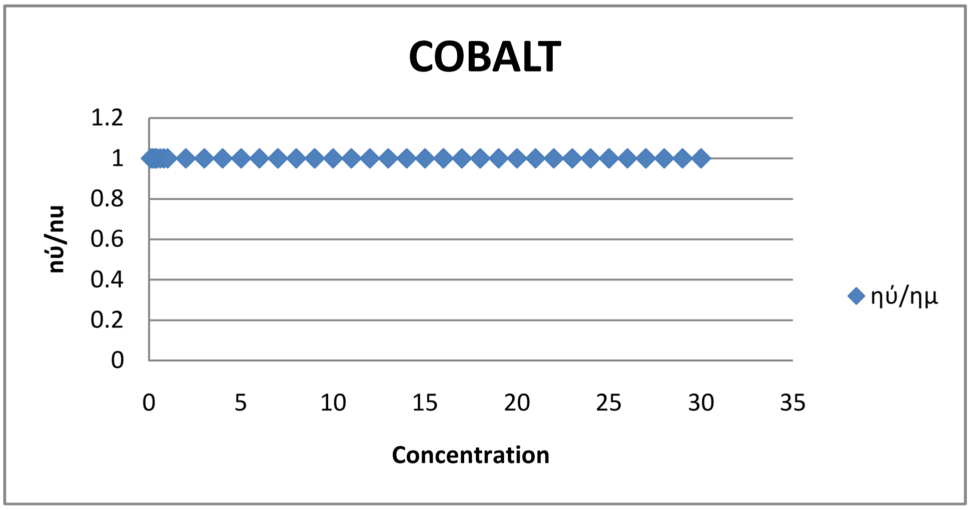

Fig 13: ηύ/ημ of Cobalt Theoreticall interference with Sodium when ΔE = kt -IP (anal)

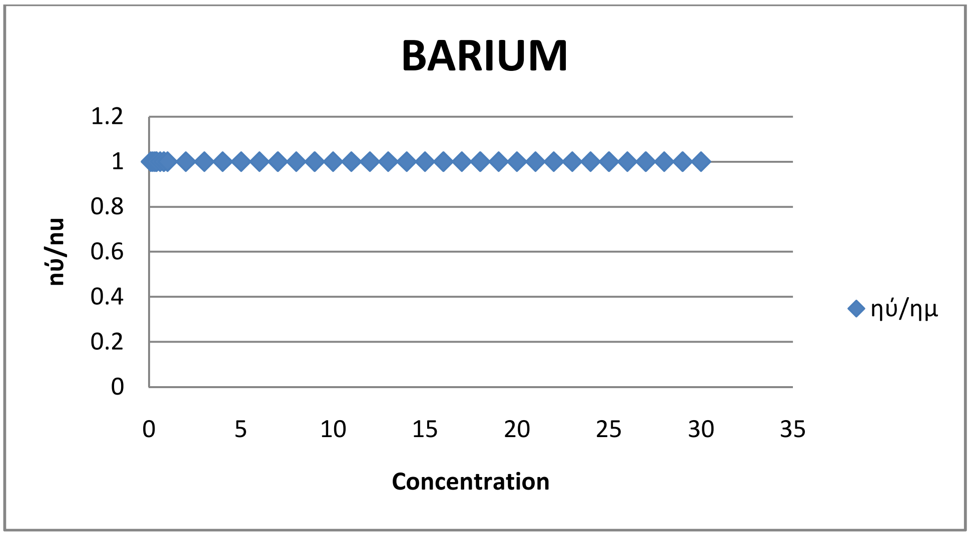

Fig 14: ηύ/ημ of Barium Theoreticall interference with Sodium when ΔE = kt -IP (anal)

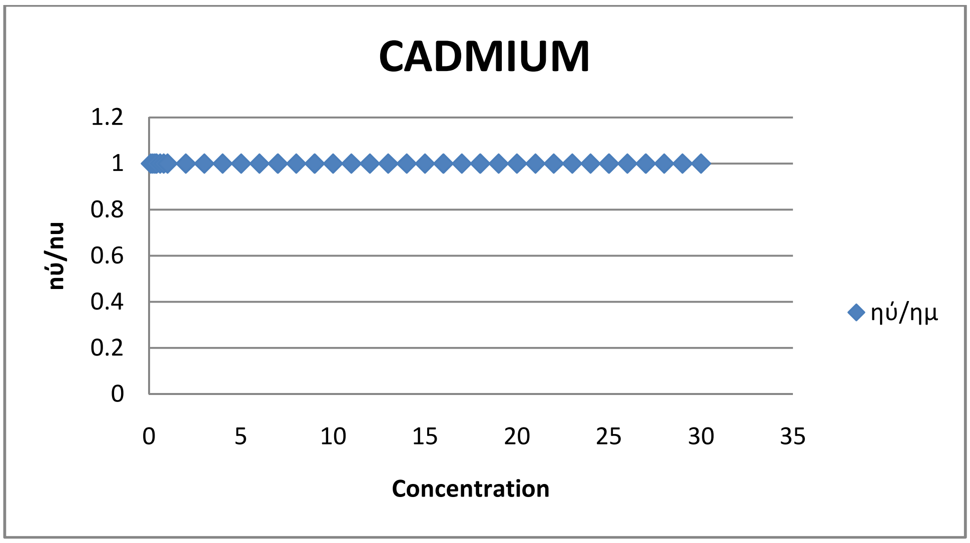

Fig 15: ηύ/ημ of Cadmium Theoreticall interference with Sodium when ΔE = kt -IP (anal)

CHAPTER 5

5.0 RESULTS AND DISCUSSION

5.1 Cobalt

5.1.1 When ΔE =0

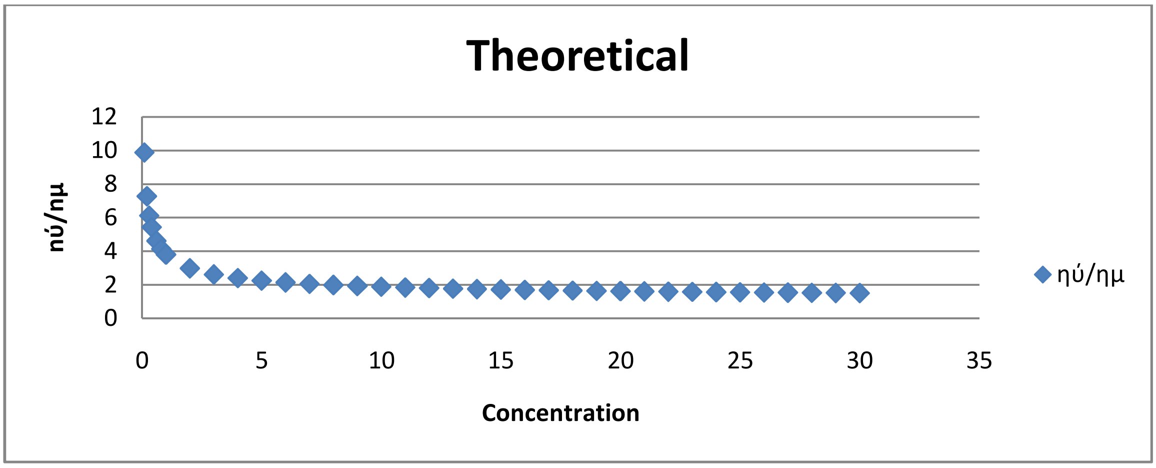

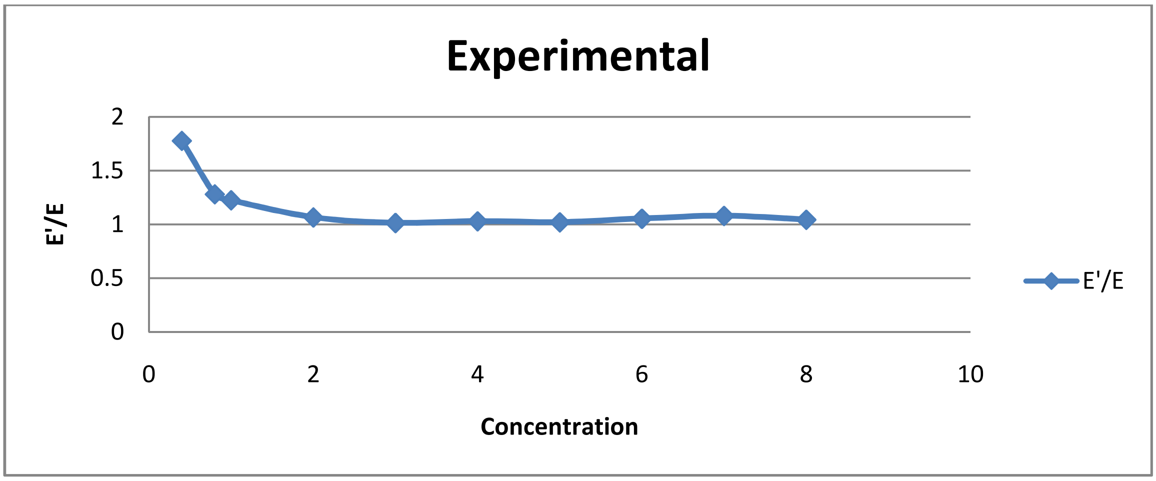

*Fig 16. Comparison between the theoretical and experimental values of Cobalt when **ΔE =0***

Fig 16 shows the comparison between the experimental and the theoretical curve of Cobalt (when ΔE =0),both the theoretical and the experimental curves show that as the concentration of the cobalt analytes decreases the effect of the sodium intereferent (1000ppm) causes an enhancement in the emission signals.Though the matching or the correlation of the graphs is not in a very close, this might have been caused by contamination of the optics as well as the purity of the NaCl salt.

5.1.2 When ΔE =IP (int) – IP (anal)

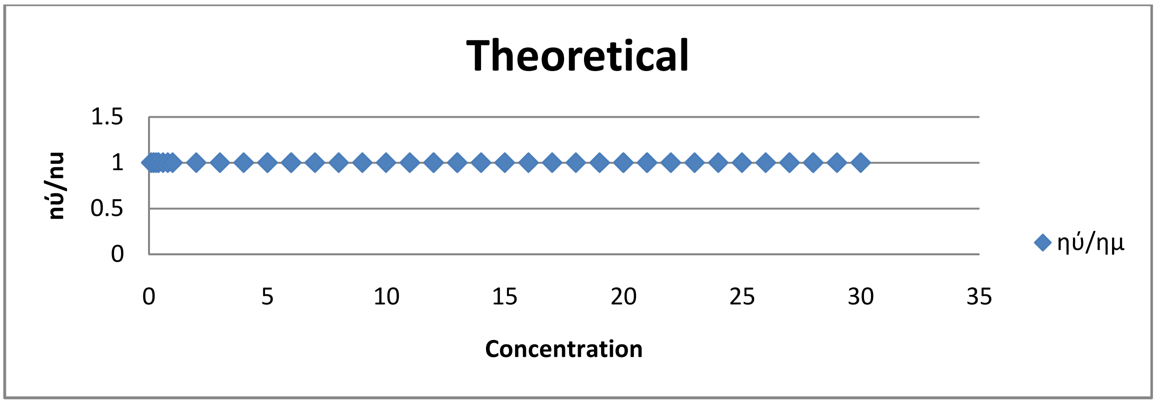

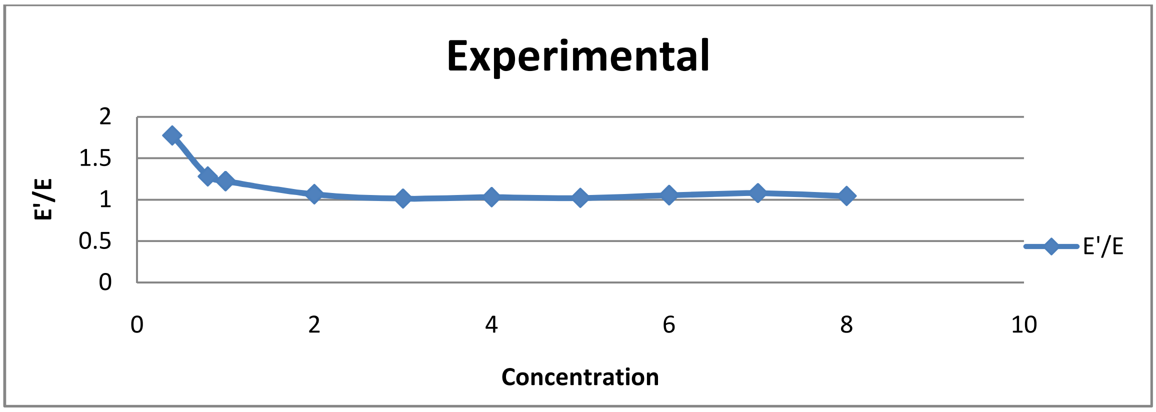

Fig 17Comparison between the theoretical and experimental values of Cobalt when ΔE =IP $_{(int)}$) – (IP $_{(anal)}$

Fig 17 shows the comparison between the theoretical and the experimental curves of Cobalt with an intereferent of 1000ppm sodium. When the assumption is that ΔE =IP $_{(int)}$ – IP $_{(anal)}$, which is the pre-LTE state, the theoretical curve shows an E'/E value of 1 which signifies that there is no change in the populations of the ground and excited states of the analytes atoms upon addition of the sodium intereferent. This contradicts with the obtained experimental curve which shows that there is E'/E values which are higher than 1showing that the assumption that ΔE =IP (int) – IP (anal) is not valid in this case.

5.1.3 When ΔE =kt –IP

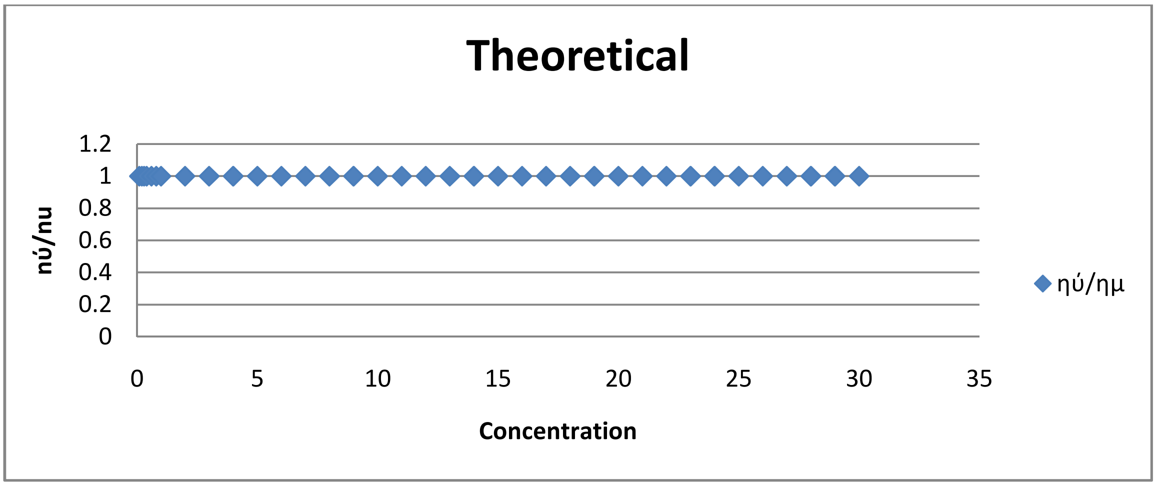

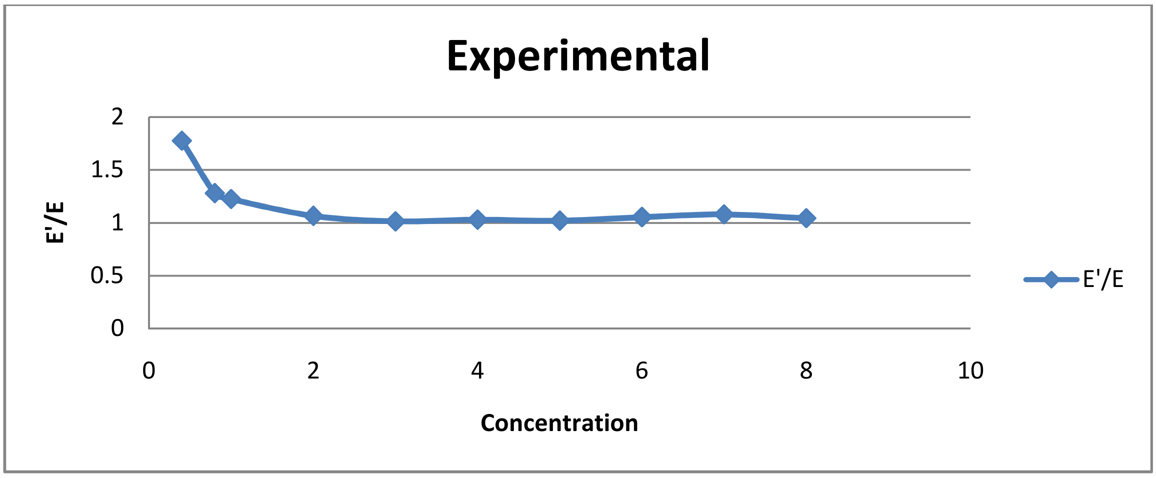

Fig 18Comparison between the theoretical and experimental values of Cobalt when ΔE =kt – IP

Fig 18 shows that the theoretically obtained curves shows no change in the populations of the ground state and the excited state as a result of the addition of 1000ppm of sodium interferent.This does not resemble the experimentally obtained curves showing that the assumption that ΔE =kt –IP (pre LTE and the LTE state) is not valid in this case.

The addition of 1000ppm of sodium intereferent to the cobalt analytes showed a significant change which is supported by the theoretically obtained curves only when ΔE =0.

5.2 Barium

5.2.1 When $\Delta E = 0$

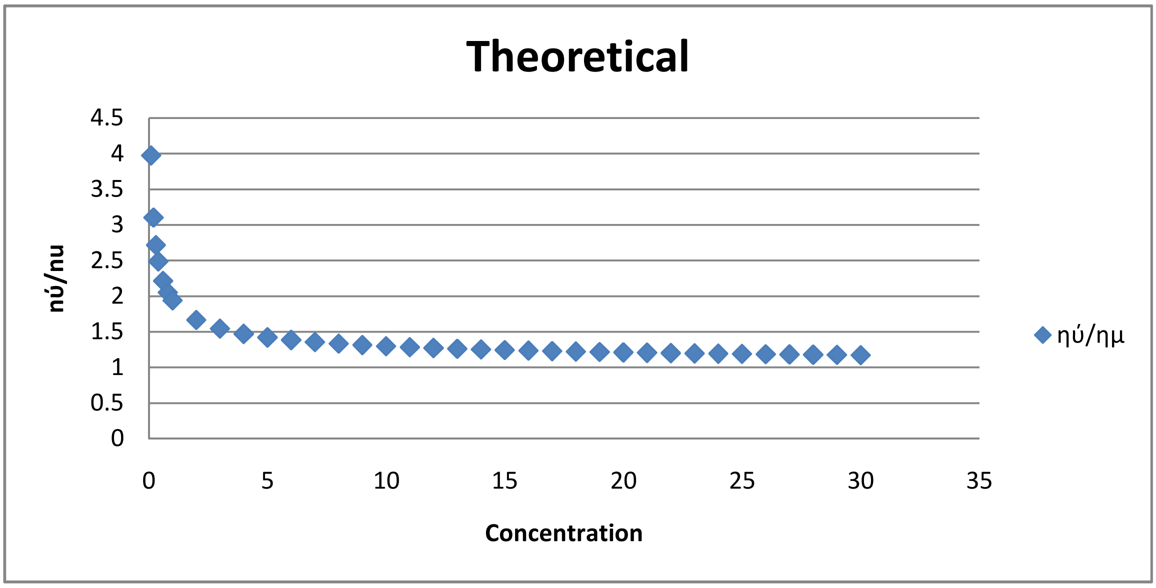

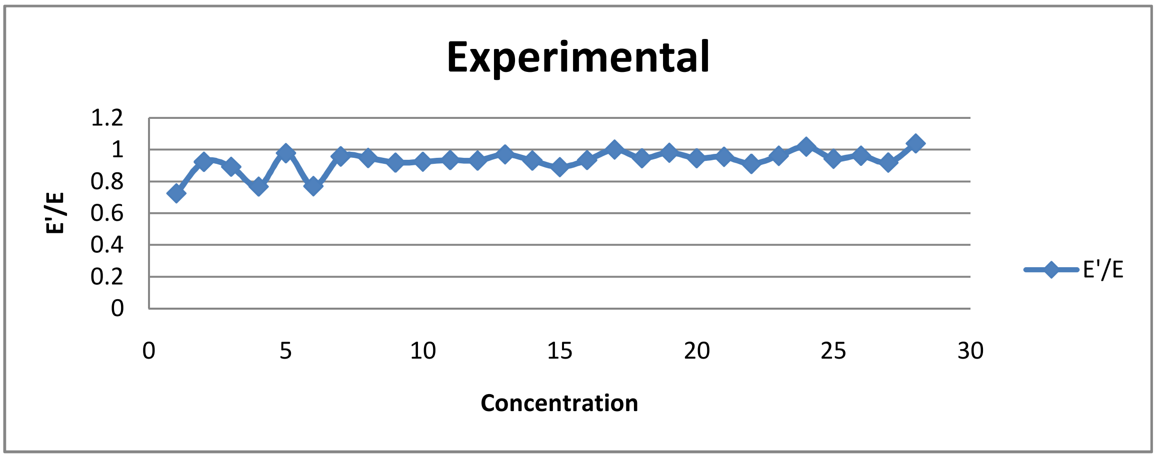

Fig 19: Comparison between the theoretical and experimental values of Barium when $\Delta E = 0$

Fig 19 shows the comparison between the experimental and the theoretical curve of Barium (when $\Delta E = 0$),the theoretical and the experimental curves differ at lower concentrations in that the theoretical curve shows an enhancement in the emission signals whereas the experimental curves reveal that the E'/E values are slightly less than 1 implying that the assumption $\Delta E = 0$ does not apply.

5.2.2 When $\Delta E = IP_{(int)} - IP_{(anal)}$

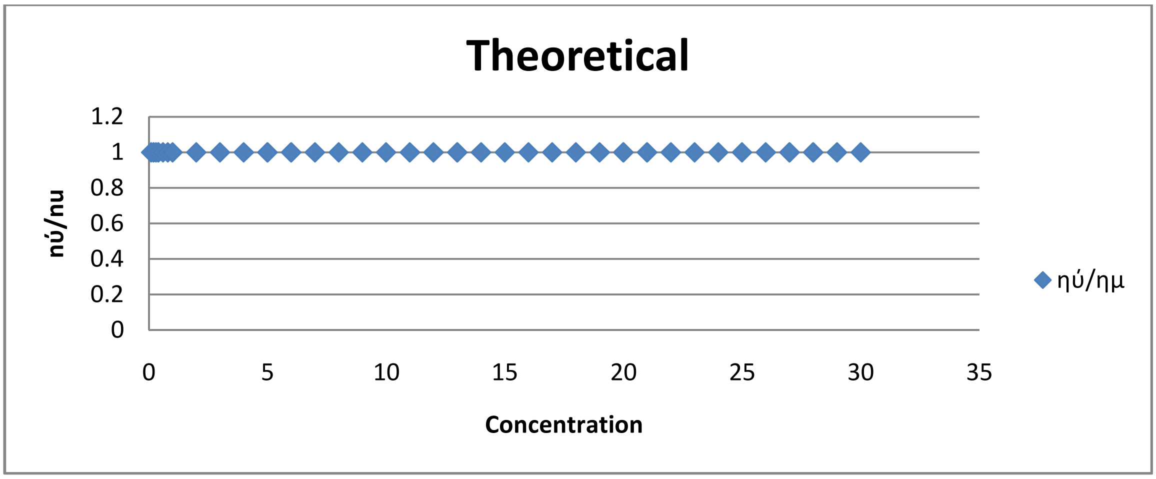

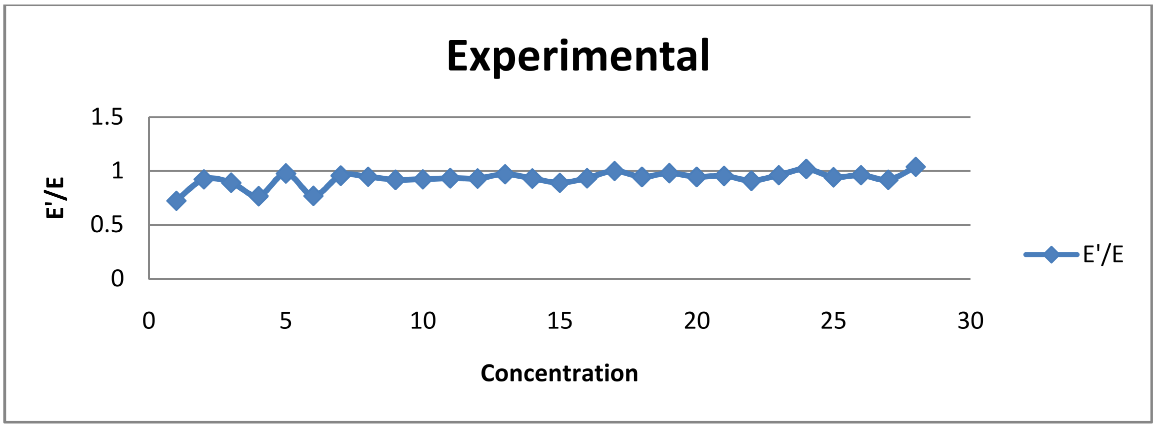

Fig 20: Comparison between the theoretical and experimental values of Barium when $\Delta E = IP_{(int)} - IP_{(anal)}$

Fig 20 shows the comparison between the theoretical curves assuming that $\Delta E = IP_{(int)} - IP_{(anal)}$ and the experimental curves derived from the analysis of Barium with 1000ppm of Sodiumintereferent. There is a close agreement between the two graphs such that the slight decrease in E'/E values of the experimental curve could be as a result of contamination. The experimental curve can be taken to resemble the assumption that $\Delta E = IP_{(int)} - IP_{(anal)}$ which gives E'/E values which are equal to 1.This means that the intereferent does not cause any matrix effects on the analysis of the Barium analytes implying that there is no change in the populations of the ground and the excited atoms.

5.2.3 When ΔE =kt –IP

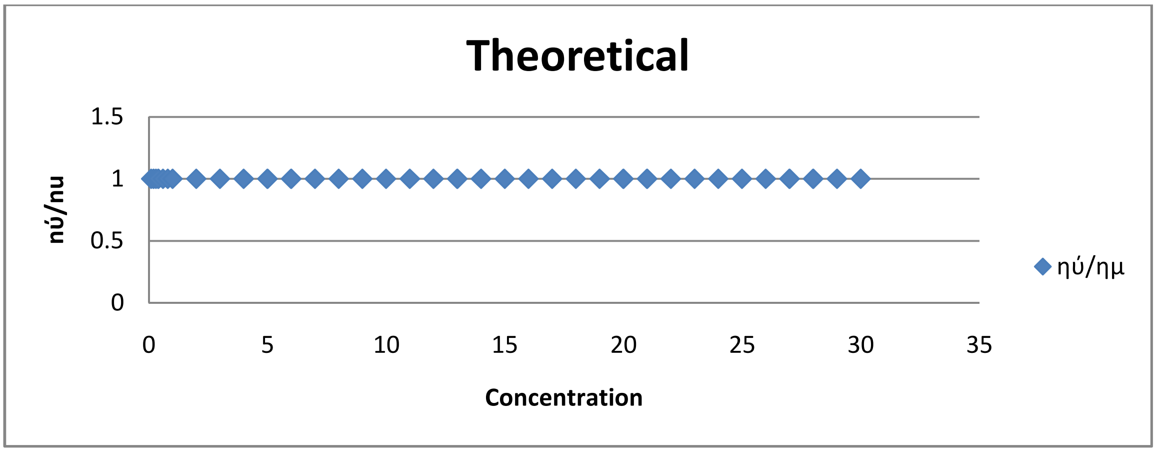

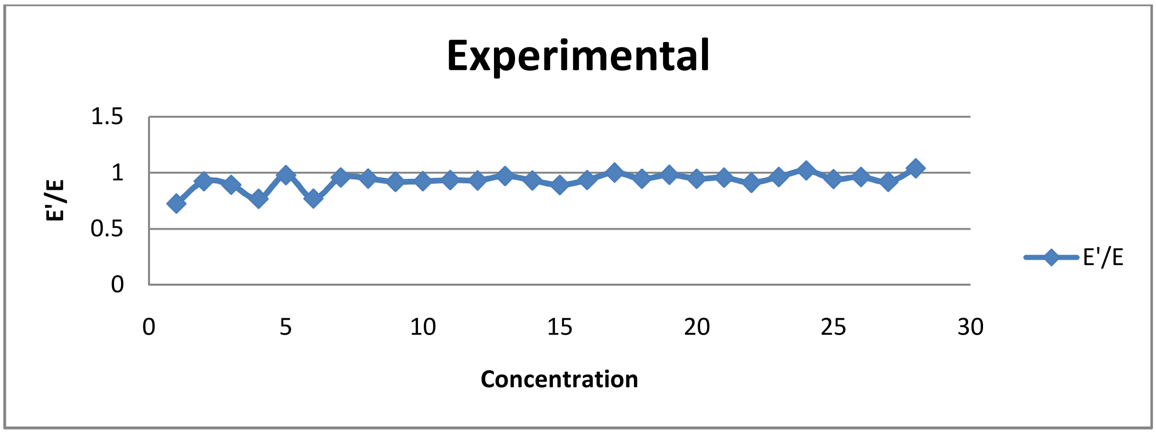

Fig21: Comparison between the theoretical and experimental values of Barium when ΔE =kt –IP

Fig 21 shows the theoretical and the experimental curves of Barium. The theoretical curve is also similar to the one in which $\Delta E = IP_{(int)} - IP_{(anal)}$ as above. This means that the intereferent does not cause any matrix effects on the analysis of the Barium analytes implying that there is no change in the populations of the ground and the excited atoms. However, this resembles both the LTE state and the pre-LTE state.

5.3 Cadmium

5.3.1 When ΔE =0

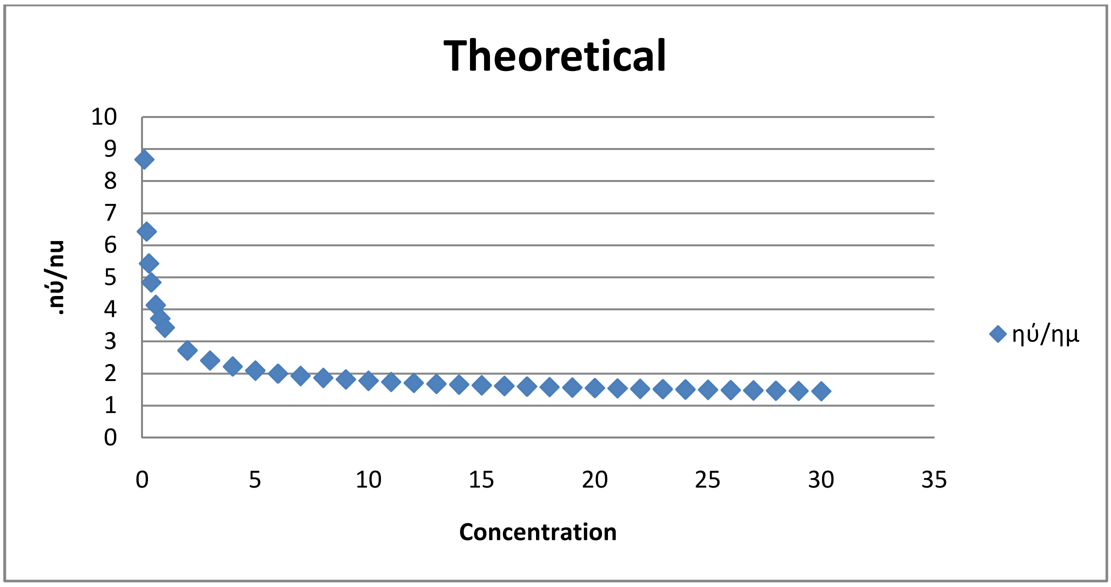

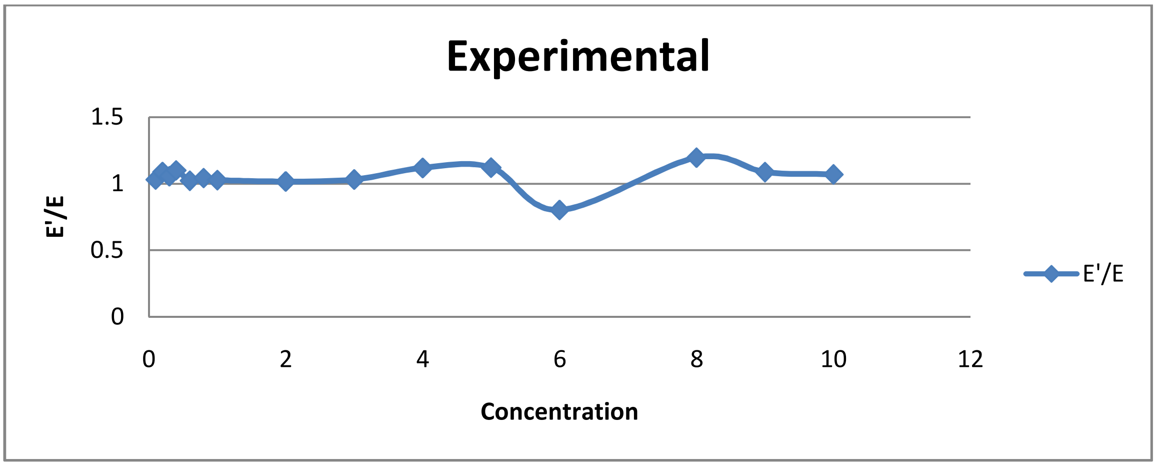

Fig22: Comparison between the theoretical and experimental values of Cadmium when ΔE =0

Fig 22 shows the comparison between the Cadmium theoretical curve and the experimentally obtained curve. The theoretical curve was obtained on the assumption that ΔE =0.The two curves do not show a consistent agreement implying that the assumption is not valid or theoretically within a close fit to the experimental curve.

5.3.2 When ΔE =IP (int) – IP (anal)

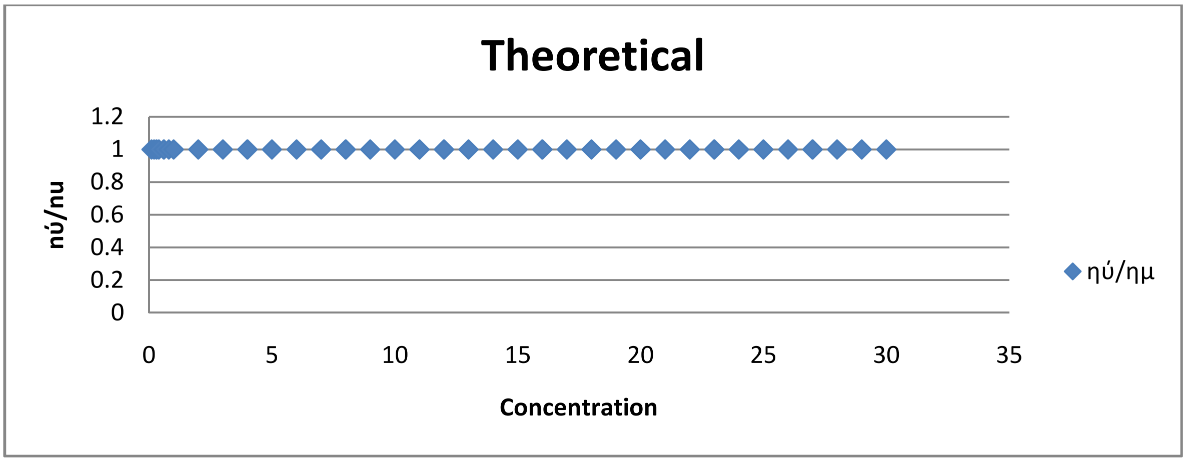

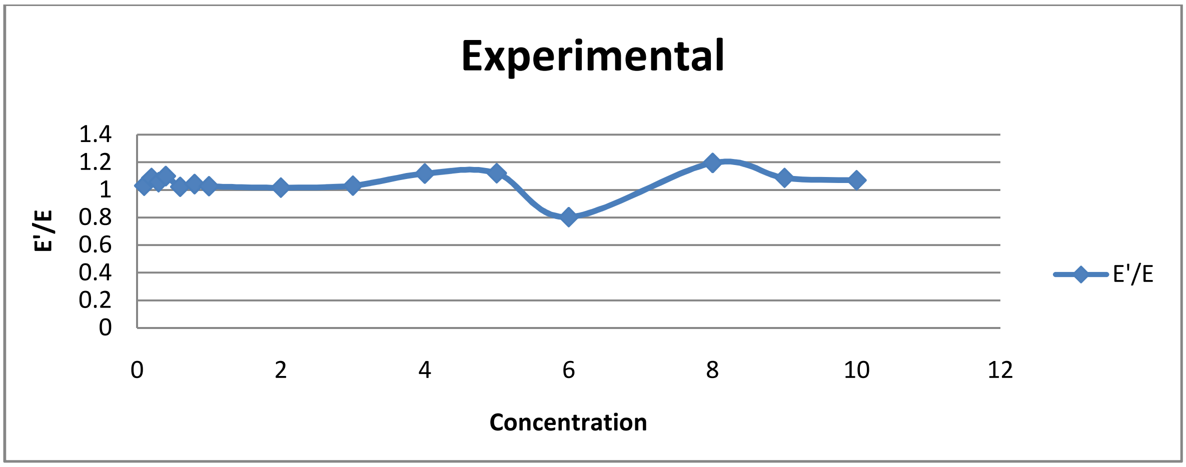

Fig 23: Comparison between the theoretical and experimental values of Cadmium when ΔE =IP (int) – IP (anal)

Fig 23 shows a comparison between the theoretical and the experimentally obtained graphs of sodium intereferent on Cadmium. There is a general similarity between the two curves suggesting that the assumption that ΔE =IP (int) – IP (anal) closely agrees with the experimental. The obtained Cadmium curve after the addition of 1000ppm could not fit with the theoretically obtained curve because of high chances of contamination of the optical lenses.

5.3.3 When ΔE =kt –IP

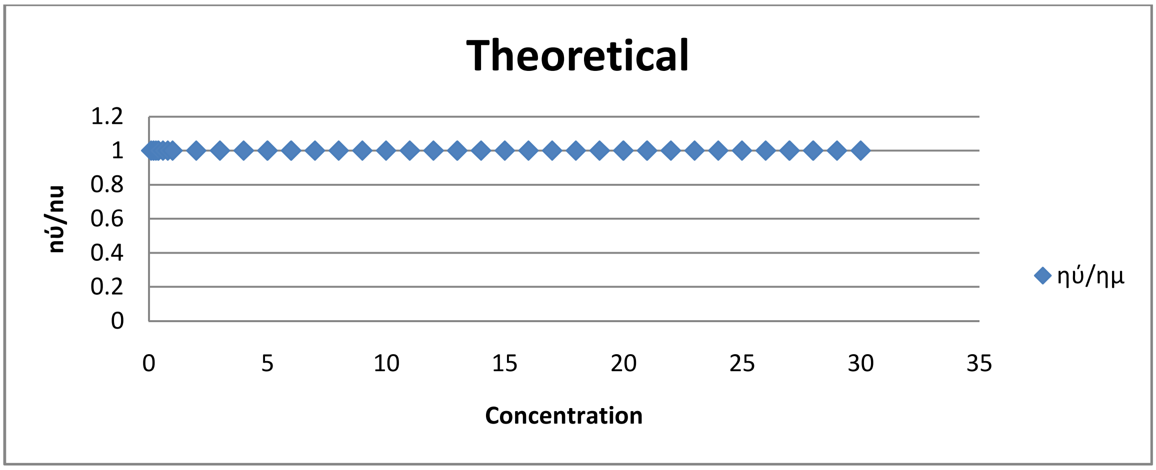

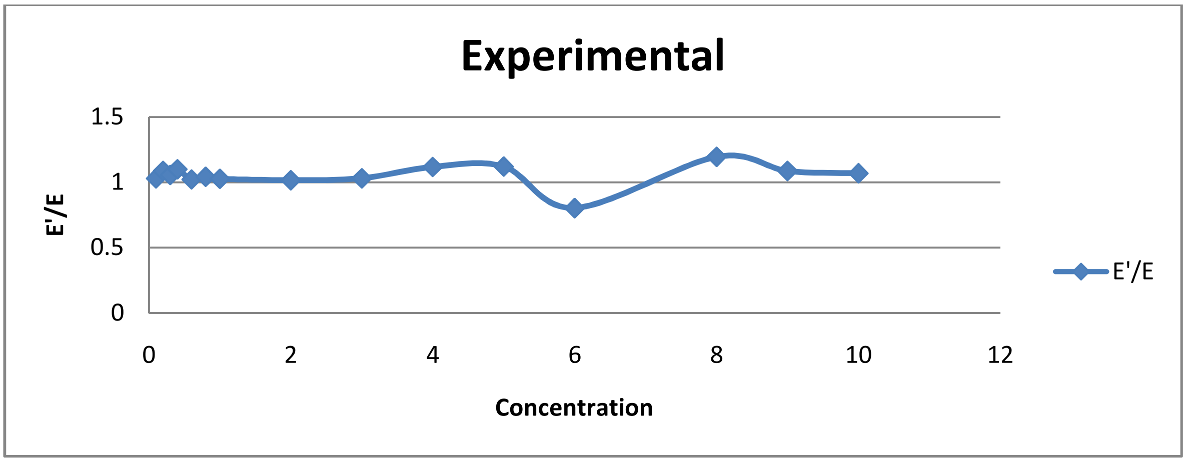

Fig 24: Comparison between the theoretical and experimental values of Cadmium when ΔE =kt –IP

The theoretical curve obtained on the assumption that ΔE =kt –IP is the same as the one obtained in Fig 23 above. There is also a closer proximity with the experimental curve implying that the assumption is also valid. Though the curve is slightly skewed toward positive E'/E values. This signifies that both states of LTE and pre-LTE exist when 1000ppm of sodium intereferent is added to Cadmium analytes.

CHAPTER

6

CONCLUSION AND RECCOMMENDATION

6.1 Conclusion

The Cobalt analytes when exposed to 1000ppm of Sodium intereferent had a close fit or similarity to the theoretical curve in which that the assumption was that ΔE =0.The obtained E'/E values were higher than 1signifying that at low concentrations there was a general enhancement of the emission signals. The possible collisional processes which took place were increase in ground state atoms as a result of the suppression of ionization and an increase in the excited state as a result of the ion-electron collisional radiative recombination.

The experimental curve of Barium, has a closer agreement to the two assumptions that $\Delta E = IP_{(int)} - IP_{(anal)}$ and $\Delta E = kt - IP$ whilst the theoretical curves gives E'/E values which are equal to 1.This means that the intereferent does not cause any matrix effects on the analysis of the Barium analytes implying that there is no change in the populations of the ground and the excited atoms.

The Cadmium analytes when exposed to 1000ppm of Sodium intereferent experimental curve, has a closer agreement to the two assumptions that $\Delta E = IP_{(int)} - (IP_{(anal)}$ and $\Delta E = kt - IP$. The theoretical curves gives E'/E values which are equal to 1.This means that the intereferent does not cause any matrix effects on the analysis of the Barium analytes implying that there is no change in the populations of the ground and the excited atoms.

The effects of EIE have been vividly seen in the analysis of cobalt in the presence of an intereferent. At very low concentrations of the analytes, the effect is very significant. This implies that during the analysis of cobalt in borehole water and well water which have very high sources of Sodium, the intereferent element correction factor (IEC) must be incorporated when setting up the method with ICP to ensure correction of the analytical result. Theoretical curves of Barium and Cadmium are not affected by the Sodium intereferent but experimentally, Barium has shown a depression in the emission signal and Cadmium exhibited a bias towards enhancement. This also requires that the IEC factor of the ICP be incorporated when analysing these elements in solution.

6.2 Recommendations

I recommend that further research be done on Ba, Cd and Co matrix interference with other EIE which are easily found in the environment such as potassium to determine the possible effects on their analysis.

Further research must also be done on other elements which have not yet been studied in relation to EIE interference with sodium and potassium. It is also recommended that the determined possible enhancement and depression be quantified to enable the determination of uncertainty values during the ICP analysis of Ba, Cd, and Co.

I also recommend that the effects of EIE on Co, Ba, and Cd be also studied using Atomic Emission Spectroscopy and a comparison be made on the extent of interference to determine the best method of analysis for the elements.

REFERENCES

Forster, H, Walter, J. N and Hume, D. N (1959), Mutual Cation Interference Effects in Flame Photometry.

Goldfarb. V. M (1981), Developments in Atomic Plasma Spectrochemical Analysis, Ed. R. M. Barnes, Heyden, London, p. 725.

Huang, M.; Hieftje, G. M, (1989) A new procedure for determination of electron temperatures and electron concentrations by Thomson scattering from analytical plasmas. Spectrochim. Acta. Part B.

Huang, M. Hieftje, G. M. Thomson scattering from an ICP. Spectrochim. Acta. Part B 1985, 40B, 1387–1400.

Huang, M. Marshall, K. A.; Hieftje, G. M. (1986) Electron temperatures and electron number densities measured by Thomson scattering in the inductively coupled plasma. Anal. Chem. 1986, 58,207–210.

Marshall, K. A.; Hieftje, G. M. Thomson scattering for determining electron concentrations and temperatures in an ICP–I: Assessment of the technique for a low-flow, low-power plasma. Spectrochim. Acta. Part B 1988, 43B, 841–849.

Nowak, S, Van Der Mullen, J. A. M and Schram, D. C (1988), Electrondensity and temperature determination in an ICP using a non-equilibriumconcept, Spectrochim. Acta 43B, (9/11), 1235-1245.

Rayson, G. D and Hieftje, G. M (1985), A steady-state approach to evaluation of proposed excitation mechanisms in the analytical ICP, Spectrochim Acta 41B (7), 683-697

Skoog D, Holler F.J, Crouch S 2007, Principles of instrumental analysis 6th Ed, Brooks/Cole United States

Standards Association of Zimbabwe ZW 560:1995 Borehole water standard.

Uchida H (1980) Measurement of metastable argon in inductively coupled plasma by atomic absorption spectroscopy. Spectrochim. Acta, 35B, 881–883.

Veillon, C. and Margoshes, M. (1968) An evaluation of the induction-coupled, radio frequency plasma torch for atomic emission and atomic absorption spectrometry." Spectrochim. Acta, 23B, 503–512.

Wendt, R.H. and Fassel, V.A. (1965) Induction coupled plasma spectrometric excitation source. Anal. Chem., 37, 920–922.

Zaranyika MF and Chirenje AT, A possible steady state kinetic model for the excitation processes during inductively coupled plasma atomic emission spectrometry: Application to interference effects of lithium on calcium, Fresenius J Anal Chem (2000), 368. 45-51

Zaranyika MF and Mahamadi C, Plasma Diagnostics through Kinetic Modelling: Characterization of Matrix Effects during ICP and Flame Atomic Spectrometry in terms of Collisional Radiative Recombination Activation Energy–A Review, J Anal Bioanal Tech 2013, Volume 4 , Issue 4

Zaranyika, M. F and Chirenje, A. T (2000).A possible Steady-state kinetic model for the atomization and excitation processes during inductively coupled plasma atomic emission spectrometry: Application to interference effects of lithium on calcium, Fresenius J. Anal. Chem., 368, 45-51.

Zaranyika, M. F, Nyakonda, C, Moses, P (1991). Effect of excess sodium on the excitation of potassium in air-acetylene flame: a steady-state kinetic model which takes into account collisional excitation. Fresenius J. Anal.Chem, 341, 577-585.

Zaranyika, M. F. and Makuhunga, P (1997), A Possible Steady State Kinetic Model for the Atomization Process during Flame Atomic Spectrometry: Application to Mutual Atomization Interference Effects between Group I Elements. Fresenius J. Anal. Chem, 357, 249-257.